Effect of inherited structural highs on the structure and kinematics of the South Dezful Embayment, SW Iran

Aref Shamszadeh[1], Khalil Sarkarinejad[1] 🔴, Oriol Ferrer[2], Soumyajit Mukherjee[3] and Mohammad Seraj[4]

[1]Department of Earth Sciences, College of Sciences, Shiraz University, Shiraz 71467-13565, Iran; [2]Institut de Recerca Geomodels, Universitat de Barcelona, Martí i Franquès s/n, Barcelona 08028, Spain; [3]Department of Earth Sciences, Indian Institute of Technology Bombay, Powai, Mumbai, Maharashtra 400 076, India and [4]National Iranian South Oil Company (NISOC), Ahwaz 61735-1313, Iran

Abstract

Understanding the structural evolution of the South Dezful Embayment (SDE) in the Zagros Fold-and-Thrust Belt (ZFTB) is significant for hydrocarbon exploration and production. The structural evolution of this area has been controlled by the reactivation of basement structures related to the oblique convergence along the ZFTB. In this work, we study the effect of the pre-contractional interaction between the basement step and overlaid salt layer superimposed by the Zagros shortening on the structural style and evolution of the sedimentary basin in the SDE. We use multidisciplinary approaches involving surface and subsurface data and analogue models. Disharmonic folds with small wavelength formed over the Kharg-Mish Palaeo-high (KMPH) where the sedimentary cover is thinner. On the other hand, faulted detachment folds with large wavelengths developed in the adjacent depocenters. Furthermore, the KMPH affected the geometry and kinematics of the frontal part of the Zagros Belt, which is characterized by the Mountain Front Flexure (MFF) topographic step. Long-lasting active deformation of the sedimentary cover over the frontal ramp of the KMPH developed the South Izeh Promontory (SIP). Localized contraction in the SIP was accommodated temporally by trishear fault-propagation folding and resulted in > 5 km elevation difference between this promontory and two adjacent local basins. Supporting scaled analogue models show that structural evolution, folding and along-strike variations in fold style of the SDE have been controlled by thickness variations of the sedimentary cover and the geometry of the inherited pre-salt structure. Based on the results of this study, the effect of inherited structural highs on the structure and kinematics of the SDE provide important insights for hydrocarbon entrapment, migration and exploration.

1. Introduction

The structural style and kinematic evolution of foreland fold-and-thrust belts become complex to understand when viscous salt in the sedimentary pile decouples deformation between the basement and the overburden. The interaction between pre-existing basement structures and the overlying salt layer is a major controlling factor in the deformation of different tectonosedimentary basins worldwide (Table 1; Misra & Mukherjee, 2015). Several studies have discussed the effect of basal décollement (Cotton & Koyi, 2000; Bahroudi & Koyi, 2003; Sherkati *et al.* 2006; Misra & Mukherjee, 2015; Farzipour-Saein & Koyi, 2016) and basement steps (Farzipour-Saein *et al.* 2013; Tong *et al.* 2014; Burberry & Swiatlowski, 2016; Lacombe & Bellahsen, 2016; Godin *et al.* 2019; Razavi Pash *et al.* 2021a) on the deformation of fold-and-thrust belts. Moreover, the spatial configuration and geometry of the deformation front of fold-and-thrust belts are affected by surface processes (sedimentation and erosion) (Storti & McClay, 1995; Koyi & Maillot, 2007; Pla *et al.* 2019) and transverse strike-slip basement fault (Hessami *et al.* 2001a; Sepehr & Cosgrove, 2004; Farzipour-Saein *et al.* 2009). However, complex geological settings in which the pre-contractional relation between the basement steps and overlaying ductile layers is affected by the subsequent shortening in fold-and-thrust belts is poorly understood.

The Dezful Embayment is one of the most productive oil provinces in the world. It contains 45 oilfields with > 360 billion barrels of oil in place and 8% of the global oil reserves (Bordenave & Hegre, 2005, 2010; Vergés *et al.* 2011). The South Dezful Embayment (SDE) in the Zagros foreland folded belt provides a good example of how the basement structural highs affect the overlying strata (Sherkati & Letouzey, 2004; Farahzadi *et al.* 2019; Noori *et al.* 2019; Vatandoust *et al.* 2020). Reactivation of Precambrian basement structures during Phanerozoic time influenced the tectonic history, geometry and deposition of the sedimentary cover (e.g. Edgell, 1992; Stewart *et al.* 2018). The Kharg-Mish Palaeo-high (KMPH), one of the main structures in the

Table 1. A summary of previous publications that have evaluated effective parameters describing the structure style of the basin

Author	Approach	Effective parameters describing the structure style of the basin	General concept	Natural example(s)
Koyi *et al.* (1993)	Analogue model/seismic reflection profile	Basement faulting, differential loading, salt layer	Yes	Dutch central graben; Gulf of Mexico; North Sea
Vendeville *et al.* (1995)	Analogue model	Salt layer and basement-involved planar extensional fault	Yes	–
Withjack & Callaway (2000)	Analogue model	Salt layer, thickness of sedimentary cover, magnitude and rate of displacement on the basement normal fault	Yes	Gulf of Suez; Haltenbanken area offshore Norway; Jeanne d'Arc Basin of the Grand Banks, offshore SE Canada
Dooley *et al.* (2005)	Analogue model	Salt diapirs and intersecting basement fault systems	Yes	Central Graben, UK North Sea
Callot *et al.* (2012)	Analogue model	Pre-existing salt diapirs	–	Zagros Fold-and-Thrust Belt, Iran
Ferrer *et al.* (2012, 2014)	Analogue model/seismic reflection profile	Salt layer and kinked-planar fault geometry at depth	Yes	Parentis Basin, Eastern Bay of Biscay
Jahani *et al.* (2017)	Seismic reflection profile	Deep-seated extensional faults and salt layer	–	Central part of Zagros Fold-and-Thrust Belt, Iran
Roma *et al.* (2018)	Analogue model	Extensional ramp/flat faults system, pre-kinematic salt	–	Columbrets Basin, western Mediterranean
Caër *et al.* (2018)	Numerical model, analogue model	Pre-existing normal fault	Yes	Jura Fold-and-Thrust Belt
Stewart *et al.* (2018)	Seismic reflection profile	Pre-existing basement structure, basal salt layer	–	NE of Arabian Plate, Persian Gulf
Borderie *et al.* (2019)	Analogue model	Influence of a basement slope at the base of the viscous décollement layer	–	Chazuta Thrust in the Huallaga Basin, Peru
Espurt *et al.* (2019)	Field-based observations/cross-section	Pre-existing salt structure and basement inheritance	–	Eastern Provence Fold-and-Thrust Belt, SE France
Dooley & Hudec (2020)	Analogue model	En échelon graben-bounding fault systems, salt layer	Yes	Moroccan High Atlas
Husseini *et al.* (2021)	Seismic profile/2D structural restorations	Basement faulting, differential loading, salt layer	–	Nordkapp Basin, Barents Sea
Schori *et al.* (2021)	Analogue model	Pre-existing basement faults	–	Jura Mountains Fold-and-Thrust Belt

SDE, is a gently elongated N–NE-trending basement structure extending to the Iranian sector of the NW Persian Gulf (Stewart, 2018; Farahzadi *et al.* 2019). It has been proposed that reactivation of the KMPH during Phanerozoic time has controlled the lateral facies changes and overburden thickness variations in the SDE (McQuillan 1991; Motiei, 1994, 1995; Sherkati & Letouzey, 2004).

In this article, we address three main issues: (i) the impact of the basement structural high on the geometry and thickness variation of the overlaying sedimentary pile in the SDE; (ii) how the KMPH controlled the structural style and folding of the SDE; and (iii) how the pre-contractional configuration of the KMPH affected the spatial variation and the geometry of the deformation front of the Zagros fold-and-thrust belt. We utilize seismic and stratigraphic data from > 300 wells, isopach maps and field observations to reconstruct the structural evolution and fold styles of the SDE. The kinematic evolution is addressed using scaled-analogue models of contractional setting with a pre-existing basement high.

2. Structures and stratigraphy

The Late Cretaceous – Palaeogene Alpine Orogeny closed the Neo-Tethyan Ocean between north Gondwana and south Laurasia margins and developed the Zagros Fold-and-Thrust Belt (ZFTB). The

belt spans *c.* 2000 km from SE Turkey to Oman (Stöcklin, 1968; Falcon, 1974; Berberian & King 1981; Alavi 1994, 2007; Vergés *et al.* 2011; Mouthereau *et al.* 2012). The ZFTB is a 25° oblique transpression zone between the Afro-Arabian continent and the Iranian microcontinent (Sarkarinejad & Azizi, 2008). The contractional reactivation of N–S- to NW–SE-trending basement structures inherited from the north Gondwana passive margin divides the ZFTB into different tectonostratigraphic zones. These basement structures are attributed to the 670–570-Ma Pan-African orogeny (e.g. Stöcklin, 1968; Sarkarinejad & Goftari, 2019).

Generally, from the NE to SW the ZFTB is divided into six main sub-parallel belts: (i) the Urumieh–Dokhtar Volcanic Arc (UDVA); (ii) Sanandaj–Sirjan Metamorphic Belt; (iii) imbricated zone; (iv) Zagros foreland Fold-and-Thrust Belt (High Zagros Belt); (v) Zagros foreland folded belt; (vi) the Mesopotamian–Persian Gulf Foreland Basin (e.g. Vergés *et al.* 2011; Sarkarinejad & Goftari, 2019; Fig. 1). The Dezful Embayment in the central part of the Zagros foreland folded belt formed in the footwall of the Mountain Front Flexure (MFF), a fault zone rooted from a NW–SE-aligned basement step, and between two transverse basement faults of the Kazerun Fault to the SE and Bala Rud to the NW (Fig. 1; e.g. Alavi, 1994; Mouthereau *et al.* 2012).
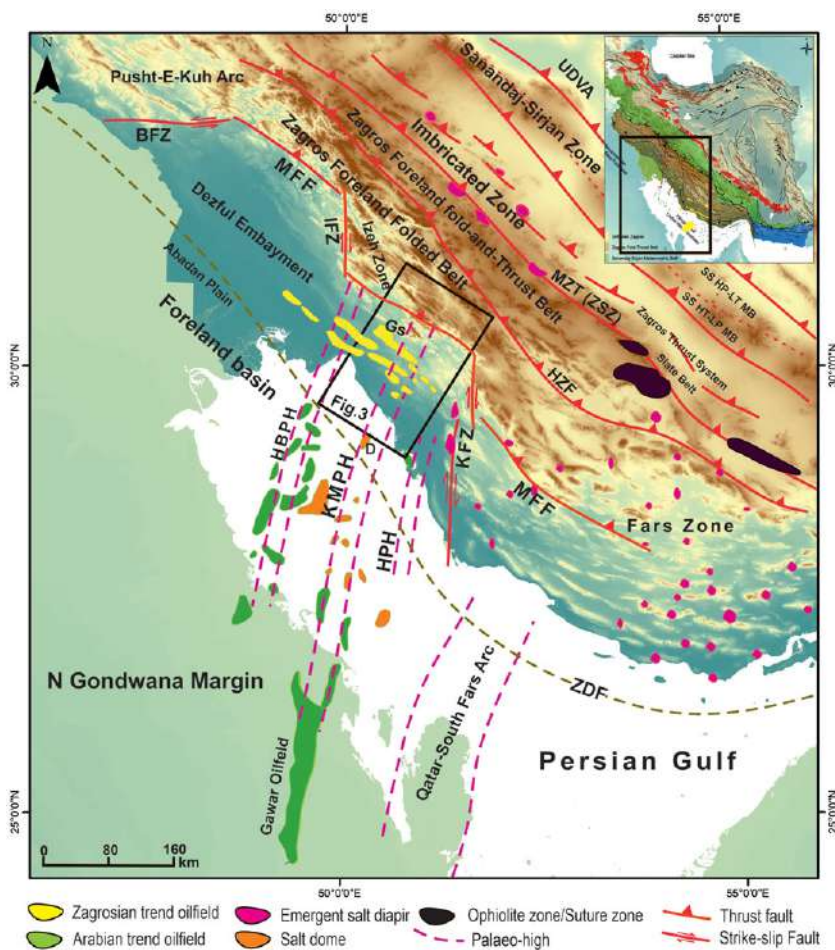
Fig. 1. (Colour online) Main structural elements of the central part of the Zagros foreland folded belt and the Zagros foreland fold-and-thrust belt. Black rectangle: study area in Figure 3. The inset map shows the location of the region on the geological map of Iran. BFZ – Bala Rud Fault Zone; D – Dorood oilfield; Gs – Gachsaran oilfield; HBPH – Hendijan-Bahregansar Palaeo-high; HPH – Helleh Palaeo-high; HZF – High Zagros Fault; IFZ – Izeh Fault Zone; KMPH – Kharg-Mish Palaeo-high; KZF – Kazerun Fault Zone; MFF – Mountain Front Flexure; MZT – Main Zagros Thrust; SS HP-LT MB – Sanandej–Sirjan high-pressure–low-temperature Metamorphic Belt; SS HT-LP MB – Sanandej–Sirjan high-pressure–low-temperature Metamorphic Belt; UDVA – Uromieh–Dokhtar Volcanic Arc; ZDF – Zagros Deformation Front; ZSZ – Zagros Suture Zone. Modified after Berberian (1995), Edgell (1996), Stewart et al. (2018), Perotti et al. (2011), Soleimany et al. (2011), Tavakoli-Shirazi et al. (2013), Jahani et al. (2017), Derikvand et al. (2018) and Sarkarinejad & Goftari (2019).

Since Proterozoic time, the Dezful Embayment has endured various tectonic events (e.g. Sherkati & Letouzey, 2004; Stewart, 2018; Stewart et al. 2018). One of the important events that occurred after the consolidation of the Arabian shield was the late Phanerozoic extensional strike-slip phase known as Najd rifting (Husseini, 1988, 1989; Talbot & Alavi, 1996; Al-Husseini, 2000; Bahroudi & Talbot, 2003). During this phase, several shallow pull-apart basins with different strikes (mainly N–S-trending) controlled the epicontinental deposition of the late Phanerozoic – early Cambrian evaporites of the Hormuz/Hormoz series (e.g. Edgell, 1996; Mukherjee et al. 2010, Mukherjee, 2011; Stewart, 2018). Several studies on the fold style and geometry of the Dezful Embayment suggest the presence of a detachment layer at the base of the sedimentary cover (e.g. Colman-Sadd, 1978; Carruba et al. 2006; Heydarzadeh et al. 2020). The outcrops of Hormuz salt in the northern border of the Izeh zone (e.g. Kent, 1979; Tavakoli-Shirazi et al. 2013; Jahani et al. 2017), and the deep-seated salt domes in Abadan plain (e.g. Edgell, 1996; Abdullahie Fard et al. 2006) and the north of the Persian Gulf close to the SDE (e.g. Edgell, 1991; Soleimany et al. 2011; Stewart, 2018), all represent further evidence of the presence of the Hormuz salt around the Dezful Embayment (Fig. 1).

Based on the limited outcrops in the High Zagros, the Hormuz basin is overlain by a shallow-marine platform environment characterized by pre-Carboniferous shale and sandstone deposits (e.g. Stampfli & Borel, 2002; Perotti et al. 2011). The characteristics of Palaeozoic rocks in the study area are not specified because of the lack of outcrops and well data.

Due to the vast Carboniferous unconformity (e.g. Faqira et al. 2009; Asl et al. 2019) as a result of Hercynian orogeny in the north Gondwana margin, Cambrian–Carboniferous thicknesses and tectonostratigraphy are unclear (e.g. Konert et al. 1999; Stewart, 2018). The Hercynian orogeny locally eroded the Palaeozoic mega-sequence resulting in the direct deposition of Permo-Mesozoic rocks over the basement (e.g. Faqira et al. 2009; Riahi et al. 2021). Permo-Triassic sea progression is determined by the deposition of basal red conglomerates and sandstones of the Faraghan Formation (Alavi, 2007). The opening of the Neo-Tethyan Ocean during the Permo-Triassic separated the north Gondwana margin to the SW from the south Laurasia margin to the NE. During this period, very shallow-marine carbonates of the Dalan and Kangan formations (Dehram Group), one of the main gas reservoirs in the ZFTB, were deposited in the NE passive margin of the Afro-Arabian Plate (Alavi, 2004; Sepehr & Cosgrove, 2004). Extensional passive margin faults of the north Gondwana margin led to a NW–SE-trending facies boundary at the rifting stage, in which the Dashtak evaporites formation changes to the Khanehkat carbonates formation from the Dezful Embayment towards the NE of the ZFTB (e.g. Setudehnia, 1978; Szabo & Kheradpir, 1978; Sherkati et al. 2006).

Triassic Dashtak evaporites act as the main intermediate décollement in most parts of the ZFTB during the contractional episode (Abdullahie Fard et al. 2006; Sepehr et al. 2006; Vergés et al. 2011; Motamedi et al. 2012; Najafi et al. 2014). Facies and thickness of Jurassic – Lower Cretaceous sediments vary laterally across the Kazerun and Izeh fault zones towards the Dezful

Embayment. Carbonate facies of the Surmeh Formation in the Fars zone changes to Adaiyeh, Mus, Alan, Sargelu, Najmeh, Gotnia and Garau formations in the Lurestan zone and North Dezful Embayment (e.g. Setudehnia, 1978; Farahzadi *et al.* 2019). In the study area, the Jurassic – Lower Cretaceous Khami Group including Surmeh, Hith, Fahliyan, Gadvan and Dariyan formations have been drilled by several wells. An unconformity related to the rifting of the Neo-Tethyan ocean separated this mega-sequence from Permo-Triassic sequences (Berberian & King, 1981; Koop & Stoneley, 1982; Alavi, 2007). The Albian shales of the Kazhdumi Formation, one of the most important source rocks in the ZFTB, unconformably overlie the Jurassic – Lower Cretaceous mega-sequences. This formation has an average thickness of 250 m and acts as a local décollement. Before the Turonian unconformity, a mega-sequence of carbonates including Sarvak and Ilam formations was deposited in a shallow continental shelf basin (Alavi, 2004). The first stage of the Alpine Orogeny, with the onset of ophiolitic obduction during Late Cretaceous (Turonian) time (Moghadam *et al.* 2013), created an important unconformity (Abdullahie Fard *et al.* 2006; Farahzadi *et al.* 2019). Late Cretaceous shallow-marine carbonates to continental siliciclastic deposits derived from the Zagros hinterland overlaid the Turonian unconformity (Alavi, 2004) (Fig. 2). The Late Cretaceous – Eocene marine shales, marls and marly limestones of the Pabdeh and Gurpi formations are the source rocks supplying oil to the Asmari Formation reservoir. These formations in the ZFTB and study area act as local décollement (e.g. Carruba *et al.* 2006; Farzipour-Saein & Koyi, 2016).

The Oligocene – early Miocene shallow-marine 250–450-m-thick Asmari Formation, the most important reservoir rock, covers the Pabdeh Formation in the study area (Fig. 2). The Miocene–Pleistocene Fars Group includes the Gachsaran, Mishan, Aghajari and Bakhtiyari formations as the post-collision transgressive sequence of the Zagros Orogeny with > 5000 m thickness (Pirouz *et al.* 2017). The Dezful Embayment, a late Cenozoic depocenter that experienced rapid subsidence (Allen & Talebian, 2011), contains a huge volume of Fars Group formations. These formations significantly affected the kinematics and evolution of the folds (Abdullahie Fard *et al.* 2011). Marine to continental deposits of Gachsaran Formation as caprock of the Asmari reservoir formed a major upper décollement horizon in the Zagros foreland fold-and-thrust belt (Bahroudi & Koyi, 2003; Derikvand *et al.* 2018). Overall, the thickness of the anisotropic sedimentary overburden reaches *c.* 10–12 km in the Dezful Embayment (e.g. Alavi, 2004; Derikvand *et al.* 2018). Three main décollement layers, including the late Precambrian – Cambrian Hormuz series, the Triassic Dashtak evaporites and the Oligo-Miocene Gachsaran Formation, together with several local décollements, are involved in the sedimentary sequence of the study area (Fig. 2) (e.g. O'Brien, 1950; Asgari *et al.* 2019).

3. Methodology and dataset

This study utilizes field observations, experimental modelling, and seismic and well data covering most of the study area. The seismic profiles (from the surface down to middle Palaeozoic strata) and well data (from the surface down to Lower Cretaceous strata) used in this work were provided by the National Iranian Oil Company (NIOC). About 45 post-stack time-migrated two-dimensional (2D) seismic profiles were interpreted across and adjacent to the KMPH in the SDE. Based on the well-to-seismic tie calibrated by six well check shots, seven key stratigraphic horizons that reach

down to the Fahliyan Formation (lower Cretaceous) have been considered. However, because of the poor resolution of seismic profiles and the transparent seismic facies, it is difficult to interpret most of the lines, especially at the deeper parts (see Misra & Mukherjee, 2018 for a discussion of such issues). Four seismic profiles concerning the KMPH (Line-1 and Line-2: intersect; Line-3: along-strike above; Line-4: along-strike adjacent) illustrate the structural style of the study area (Fig. 3).

More than 400 wells from the different oil fields have been used in order to construct thickness maps, well correlation profiles, longitudinal sections and well-to-seismic ties, most of which reach the Asmari Formation. The Surmeh Formation (Jurassic) is the deepest formation drilled in the area. Two stratigraphic correlations perpendicular to the KMPH were constructed using well log analyses of the Khaviz (Khz), Gachsaran (Gs), Dara (Dr), Pazanan (Pz), Kheirabad (Khb), Garangan (Gn), Chilingar (CH) and Chaharbisheh (Cb) fields (Fig. 3).

To investigate the effect of pre-salt structure on the structural style and kinematics of the study area we have used scaled 1 g analogue models as complementary data for this study. Experiments were performed in the tectonic laboratory of the Geomodel Research Institute at the University of Barcelona. Scaling assumptions of the model are similar to Mukherjee *et al.* (2012), Granado *et al.* (2017), Roma *et al.* (2018) and Reber *et al.* (2021), in which dynamic scaling was achieved through establishing model/prototype ratios for fundamental units according to the scale model theory of Hubbert (1937). Table 2 presents the main properties of the experimental material and the scaling parameters.

4. Results

4.a. The Kharg-Mish Palaeo-high

The Kharg-Mish Fault (KMF) is a N–S-trending extensional dip-slip basement fault bounding the KMPH (Fig. 3) (e.g. Sherkati & Letouzey, 2004; Soleimany *et al.* 2011). The Haleh and Hendijan-Bahregansar Palaeo-highs are located in the east and west, respectively (Fig. 1). Well correlation down to the Lower Cretaceous sediments along the Khaviz, Gachsaran and Dara oilfields clearly show a progressive thinning of the Bangestan Group towards the KMPH from *c.* 1200 m to *c.* 350 m, possibly due to syn-kinematic sedimentation or erosion (Fig. 4). Further, the section displays progressive thinning of the Asmari and Pabdeh formations towards the KMPH from *c.* 500 m and *c.* 410 m to *c.* 290 m and *c.* 120 m, respectively. Based on the Gs-227 well log, the Upper Cretaceous Ilam and Gurpi formations were either eroded completely or were not deposited over the KMPH (Fig. 4). Moreover, the flattened horizon on top of the Turonian unconformity clearly shows the significant influence of the KMPH on the lateral thickness variation of the Sarvak Formation. In this regard, the thickness of this formation reduces from *c.* 954 m at the Khz-02 well in the west to *c.* 364 m at Gs-227 well in the east (above the KMPH) (Fig. 4).

An isopach map shows that the Bangestan Group gradually thickens towards the NW across a NE–SW-trending linear feature, presumably a deep-seated dip-slip fault that acted as a depocenter (Fig. 5a). Reactivation of the N–S-trending basement faults during the Late Cretaceous ophiolite obduction might have given rise to the Turonian unconformity in the SDE (e.g. Sherkati & Letouzey, 2004; Noori *et al.* 2019). Here we also used magnetic data from the study area to delineate the structural boundaries related to the gneissic basement heterogeneity (Fig. 5b). A vertical magnetic intensity map derived from SDE magnetic data clearly traces the
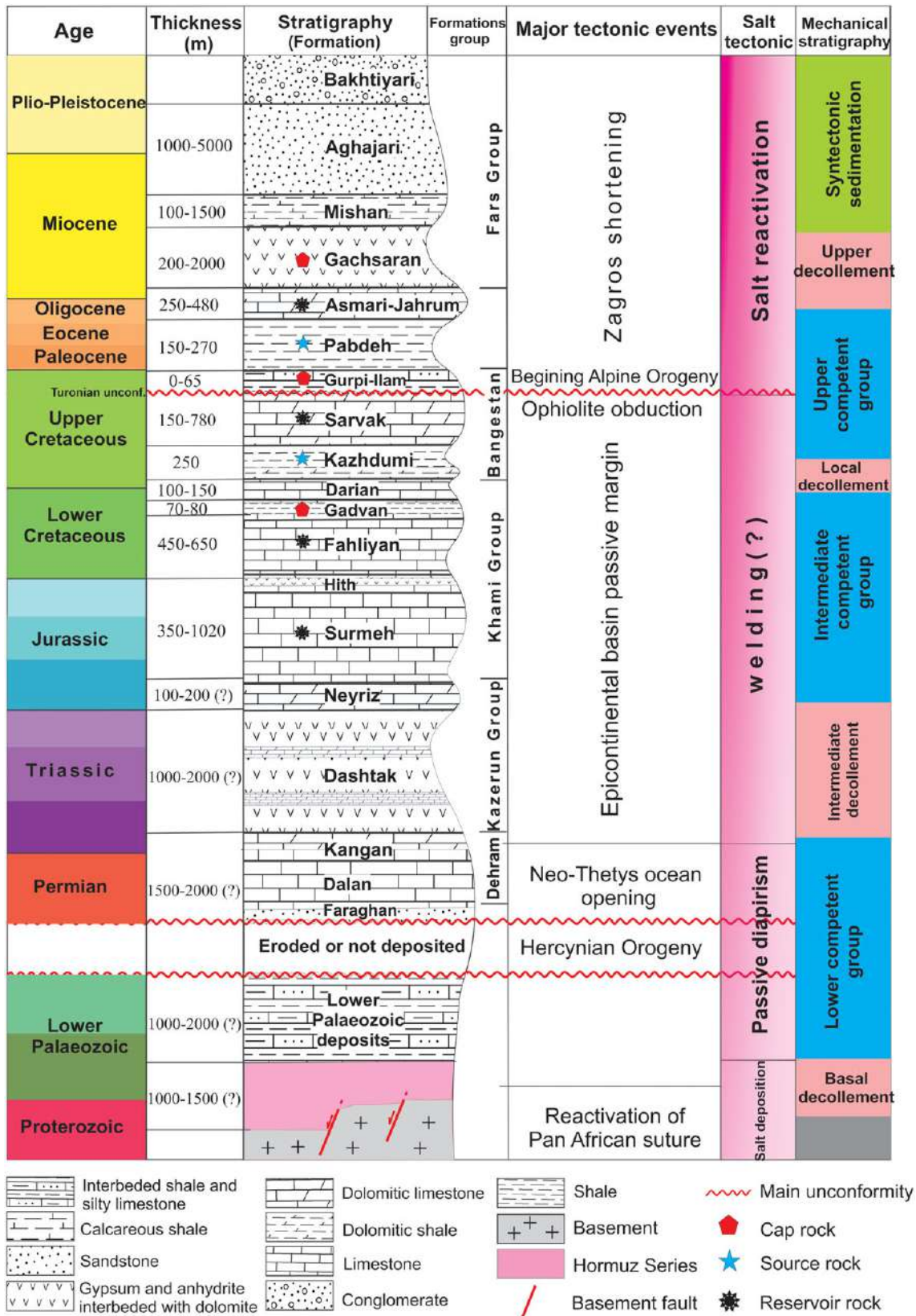
Fig. 2. (Colour online) Tectonostratigraphic column of the South Dezful Embayment based on surface and subsurface data. The right-hand-side column provides a general description of the mechanical rheology. Competent units are separated by several incompetent units acting as décollements. Modified after Alavi (2004), Sherkati & Letouzey (2004), Abdullahie Fard *et al.* (2006) and Soleimany *et al.* (2011).

Table 2. Material properties and scaled parameters used in analogue models

Parameter	Model	Nature	Model/nature ratio
Length, L	1 cm	1 km	1×10^{-5}
Gravity acceleration, g	9.81 m s^{-2}	9.81 m s^{-2}	1
Dry quartz sand density, ρ	1.6 kg m^{-3}	2.6 kg m^{-3}	0.61
Angle of internal friction, ϕ	34.6°	30–40°	1.1–0.8
Density of polymer, ρ	0.97 g cm^{-3}	2.2 g cm^{-3}	0.44
Viscosity of polymer, η	10^4 Pa s	10^{19} Pa s	1×10^{-15}
Velocity, v	8 mm h^{-1}	20 mm a^{-1}	3.5×10^3
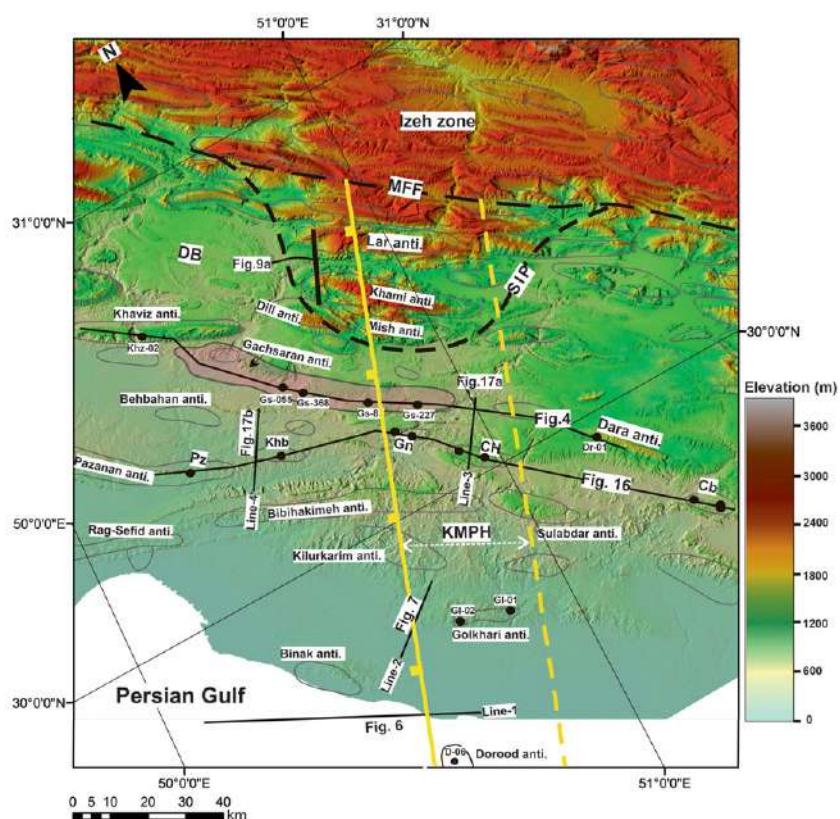
Fig. 3. (Colour online) DEM of the study area with the main structural elements (see Fig. 1 for regional location). Yellow dashed and solid lines: KMPH borders; black dashed lines: Mountain Front Flexure (MFF) and SIP. Gachsaran oilfield highlighted in pink. CH – Chilingar field; Cb – Chahar–Bisheh anticline; DB – Dehdasht Basin; Gn – Garangan field; Khb – Kheirabad Field; KK – Kilurkarim structure; Pz – Pazanan field; SIP – South Izeh Promontory.

KMPH (Fig. 5b). A comparison between isopach and vertical magnetic intensity maps of the area reveals a good match in terms of trend and overall location of the KMPH (Fig. 5).

Although the origin of the KMPH has already been described by the reactivated basement faults (e.g. Motiei, 1994, 1995; Farahzadi *et al.* 2019), no deep-seated fault trace has been interpreted along-strike of the KMPH in the sedimentary cover (Fig. 6). Because of the low-resolution 2D seismic profiles, it is difficult to interpret the basement structure. Seismic profiles across the western edge of the KMPH in the southern part of the SDE indicate a subsurface anticlinal structure (Fig. 6). The shape and geometry of this structure and its related depocenter suggest that it is a salt-related structure (Soleimany *et al.* 2011) and probably controlled by a deep-seated fault in the gneissic basement (Fig. 6). This structure has a wavelength of *c.* 12 km with gentle dips at the top of the Bangestan Group (Fig. 6).

Folds below the Bangestan Group are tighter than those in the younger strata (Fig. 6). The variable thickness of sedimentary layers near the flanks of the structure are clearly visible (Fig. 6).

Despite the significant thinning of the Late Cretaceous sediments, Pabdeh-Gurpi and Asmari formations are still thin towards the KMPH. On the other hand, the geometry and thickness (*c.* 2500 m) of the Upper Triassic (Dashtak top) to Upper Cretaceous sediments are uniform across the KMPH. Another clear variation in the thickness is indicated in the strata at the top of the Aghajari and Bakhtiyari formations (Fig. 6).

In Line-2, the geometry of the Golkhari anticline in the western margin of KMPH displays a salt-cored structure detached from the Hormuz salt layers (Fig. 7). Layer-parallel shortening related to the Zagros deformation front has caused slight vergence of this structure to the SW (similar to fore-folds) with the development of a fore-thrust (Fig. 7). This structure cannot be considered to be a normal drag fold since the layer away from the fault is also warped (Mukherjee, 2014). The structure of line-1 (Fig. 6) has been less affected by the shortening of the Zagros Orogeny, where some growth strata above the Aghajari and Bakhtiyari formations have been ascertained.
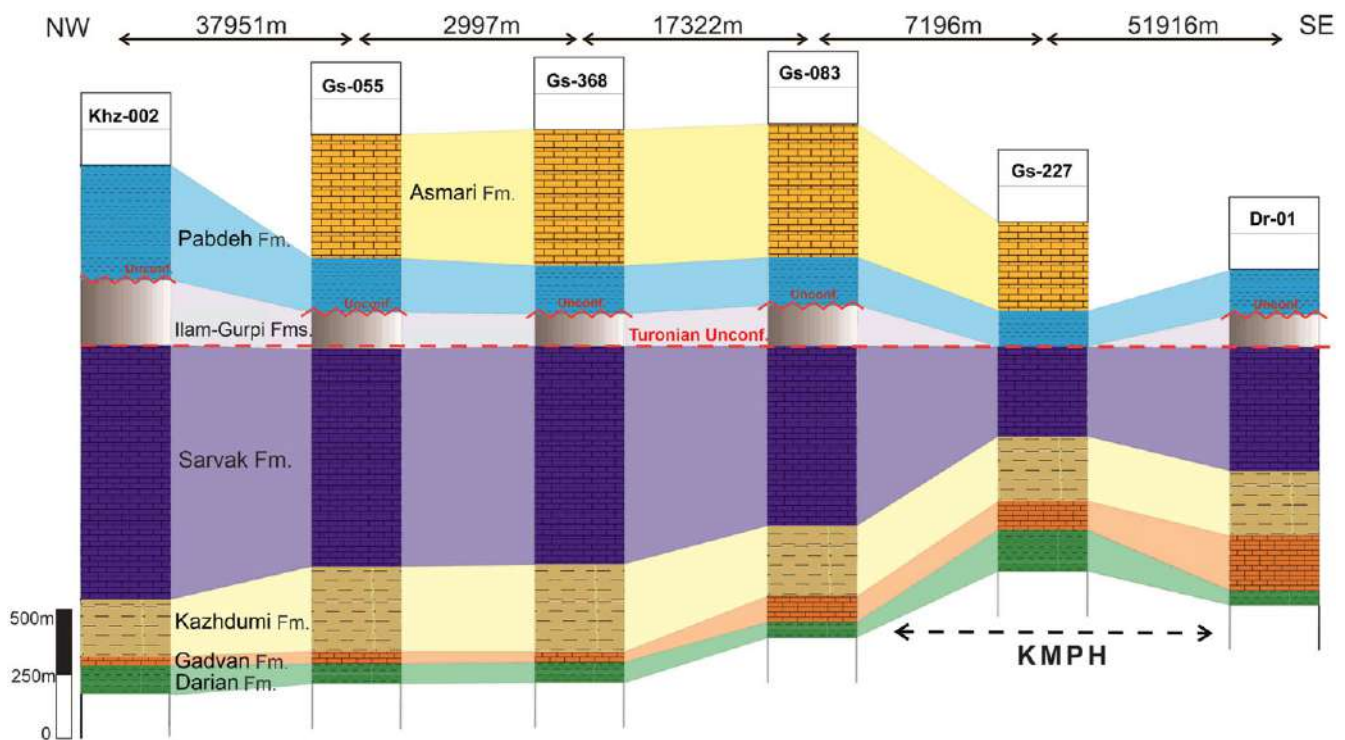
Fig. 4. (Colour online) Well correlation profile across the Khaviz, Gachsaran and Dara oilfields in the South Dezful Embayment (see Fig. 3 for location). The stratigraphic section is perpendicular to the Kharg-Mish Palaeo-high trend. Khz – Khaviz Field; Gs – Gachsaran field; and Dr – Dara field.

## 4.b. Mountain Front Flexure (South Izeh Promontory)

The Mountain Front Flexure (MFF) corresponds to a topographic step in the frontal part of the Zagros foreland folded belt. This structure is determined by active anticlines related to branched thrusts and back-thrusts in the outcrop (Fig. 8). The magneto-stratigraphic studies of the NW of ZFTB have determined the long-lasting activity of the MFF during 8.1–7.2 Ma, to around the Pliocene–Pleistocene boundary (Hessami *et al.* 2001*b*, 2006; Homke *et al.* 2004). Several constructed cross-sections of the ZFTB demonstrate that the uplift of the MFF is related to basal detachment accumulation in the base of sedimentary cover (e.g. Hessami *et al.* 2001*b*; Hinsch & Bretis, 2015). However, based on seismologic data and the different structural elevations of the sedimentary cover, other researchers have interpreted the MFF as a major blind thrust or a reactivated basement fault (e.g. Berberian, 1995; Tavani *et al.* 2020). Seismicity in this area confirms the MFF to be active (Jassim & Goff, 2006; Karasözen *et al.* 2019; Zebari *et al.* 2019). The review of the seismic evidence along the MFF supports the theory that most of the earthquakes occurred within the sedimentary cover rather than in the basement (McQuarrie, 2004). Dill, Mish, Khami and Lar anticlines, the outermost anticlines of the Izeh zone (South Izeh Promontory, SIP), steeply plunge NW-wards into the Dehdasht Basin (Fig. 8a). These anticlines are located along the trace of the KMPH. The development of the structures of the SIP was accompanied by several landslides (Fig. 8a, d). The most external folds of the SIP, the Mish anticline, is located to the north of the Gachsaran oilfield. This anticline is geometrically characterized by an overturned forelimb including the Asmari, Pabdeh and Gurpi formations. High uplift along the MFF has placed these formations over the Pleistocene conglomerates of the Bakhtiyari Formation in the SDE (Fig. 8c, d).

4.c. Experimental results

4.c.1. Initial stage and procedure

An experimental programme consisting of six experiments was developed to understand the kinematic and structural evolution of the SDE. Here, we present the results of the final model to compare with the structure of the area. The thickness and mechanical stratigraphy of the models were scaled according to the mechanical stratigraphy of the SDE (Fig. 9a). A rigid wooden block attached to a fixed wall and located at the central part of the experiments simulates the KMPH (Fig. 9b). This structural high was slightly oblique to the shortening direction ($\beta = 5°$) so that the oblique shortening direction (σ_1) of the Zagros Orogeny concerning the KMPH trend (c. 5°) is replicated (e.g. Zarifi *et al.* 2014).

The basal plate was covered by a 1.3-cm-thick blue polymer layer, which lies 3 mm above the structural high. Polydimethylsiloxane (PDMS), a see-through polymer, was used as an analogue of basal salt. PDMS (Rhodia Rhodorsil Gum FB) has near-perfect Newtonian fluid behavioural properties at a laboratory strain rate of 1.83×10^{-4} s^{-1} at 20 °C; (Weijermars, 1986; Mukherjee *et al.* 2012; Dell'Ertole & Schellart, 2013), with a density (ρ) of 972 kg m^{-3} and a dynamic viscosity (η) of 10^4 Pa s. Once the polymer was completely flat, it was overlaid by a 6-mm-thick white sand layer. Layered white and coloured (blue, red, green and brown) quartz sands with an average grain size of 250 µm, an angle of internal friction of 34.6°, a bulk density of 1500 kg m^{-3}, a coefficient of internal friction of 0.69 and a low apparent cohesive strength of 55 Pa (measured with a ring shear tester at the Fault Dynamic Analogue Modelling Laboratory of the Royal Holloway University of London) were used to simulate the brittle behaviour of the upper continental crust (see also Granado *et al.* 2017; Roma *et al.* 2018). Furthermore, following Warsitzka *et al.* (2015), lateral polymer flow was forced by adding a sand wedge
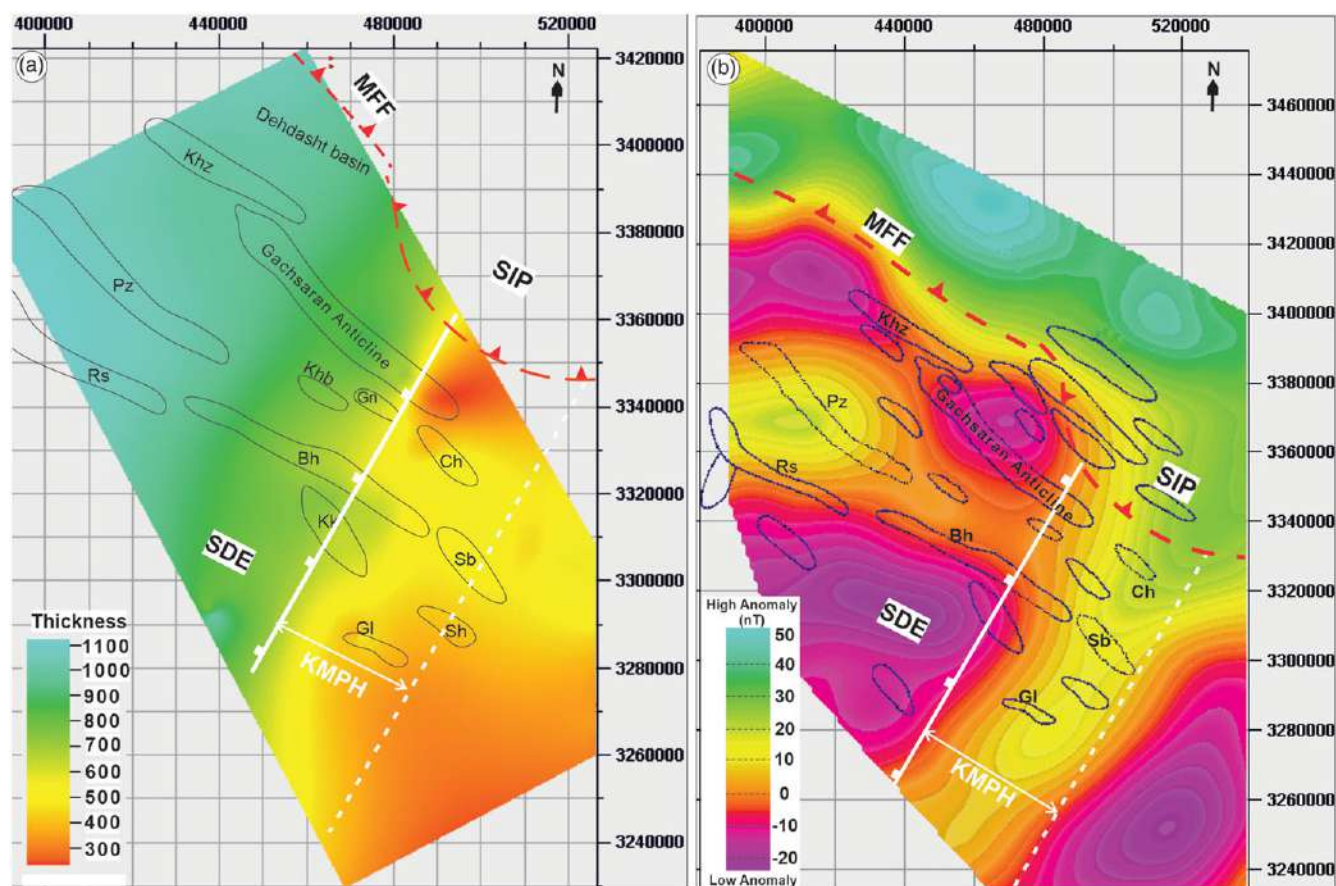
Fig. 5. (Colour online) (a) Bangestan Group isopach map of the SDE. (b) Vertical magnetic intensity map derived from magnetic data of the South Dezful Embayment. Projected coordinate system (UTM) was applied to the maps. SIP – South Izeh Promontory; Pz – Pazanan anticline; Rs – Rag-e-Sefid anticline; Bh – Bibihakimeh anticline; KK – Kilurarim anticline; Sb – Sulabdar anticline; Sh – Shur anticline; Gl – Golkhari anticline; Ch – Chilingar anticline; Gn – Garangan anticline; Khb – Kheirabad anticline; Khz – Khaviz anticline; MFF – Mountain Front Flexure.

covering both sides of the structural high and the hinterland (Fig. 9c(1)). Polymer flow was enhanced by successive sand layers deposited at intervals of 8 hours, producing inflation above the structural high. Once the polymer layer was depleted below the main depocenters adjacent to the structural high (Fig. 9c(2)) the experiment was covered by layers of sands and microbeads before beginning shortening (Fig. 9a). Glass microbeads with an average grain size of 90 μm and an internal friction coefficient of 0.37 (Koyi & Vendeville, 2003) were used to simulate the Dashtak and Kazhdumi formations (the middle décollements) in the study area.

4.c.2. General features

Figure 10 shows the structural style and geometry of the structures at the end of the shortening across the entire model. The model shows along-strike variation of the structures where the basal plate structurally defined two main deformation domains (Fig. 10). Four x-line sections, parallel to shortening direction, have been presented to demonstrate different geometries over and adjacent to the pre-existing structural high (Fig. 10c). Two different structural styles constrained by the salt thickness/structural high can be identified: (i) different thrust and back-thrust bounding large pop-up structures develop at both sides of the structural high where the salt layer was depleted before shortening (Fig. 10c, x-lines 1 and 4); and (ii) salt-cored anticlines or salt-inflated areas, closely-spaced thrusts and back-thrusts and smaller pop-up structures with

different degrees of shortening rate developed above the structural high where the salt layer was thicker before shortening (Fig. 10c, x-lines 2 and 3). Different geometries for the salt anticlines over the frontal ramp of the structural high (T2-1) can be observed along-strike the structure towards the adjacent depocnters (T2-2 and T2-3, Fig. 10). The depth slice maps show how the geometry of the deformation front (T2-1, T2-2 and T2-3) varies from the centre towards the adjacent area (Fig. 10a, b).

The topography profile of x-line sections along the basal plate and adjacent depocenters at the end of the experiment are depicted in Figure 11. The results indicate that the topography profiles along the basal plate (x-lines 2 and 3) are located at a higher level than the adjacent depocenters (x-lines 1 and 4). In addition, the difference in deformation front propagation (c. 3.5 cm) between two areas has been determined by the topography profiles. These profiles explain the local high elevation and propagation of the salt-cored anticline over the frontal ramp of the structural high (Fig. 11a, b).

4.c.3. Kinematic evolution

Figure 12 demonstrate how step-wide deformation progressed in the model in several steps. At shortening of 3–5 cm, a thrust verging towards the foreland develops parallel to the moving wall (T1 in Figs 12a, 13a–c). A gentle and symmetric anticline begins to rise, indicated by the inflated polymer at the boundary of the inherited structural high closer to the moving wall (Fig. 12a). At this point the structural high acts as a passive indentor inhibiting the
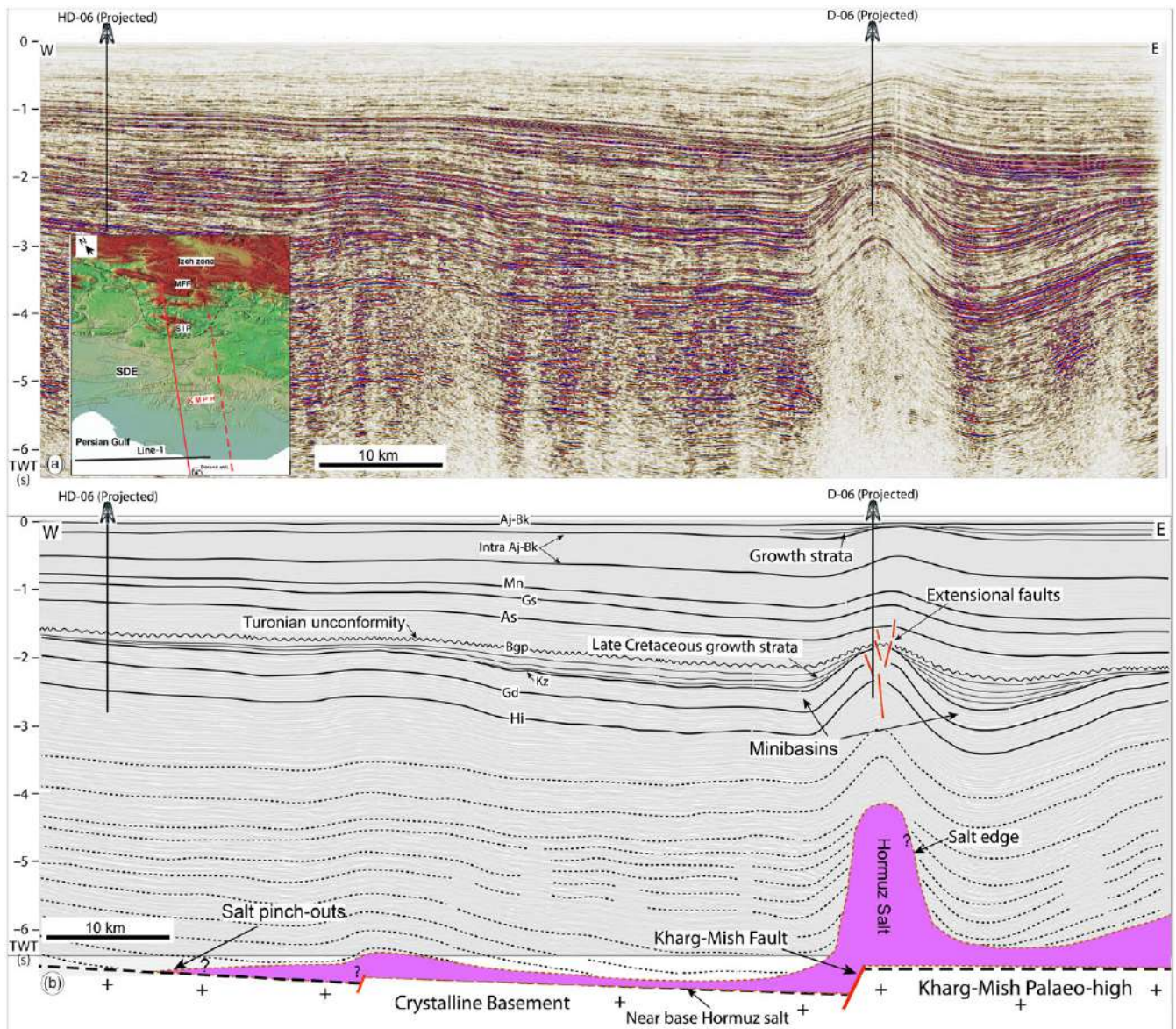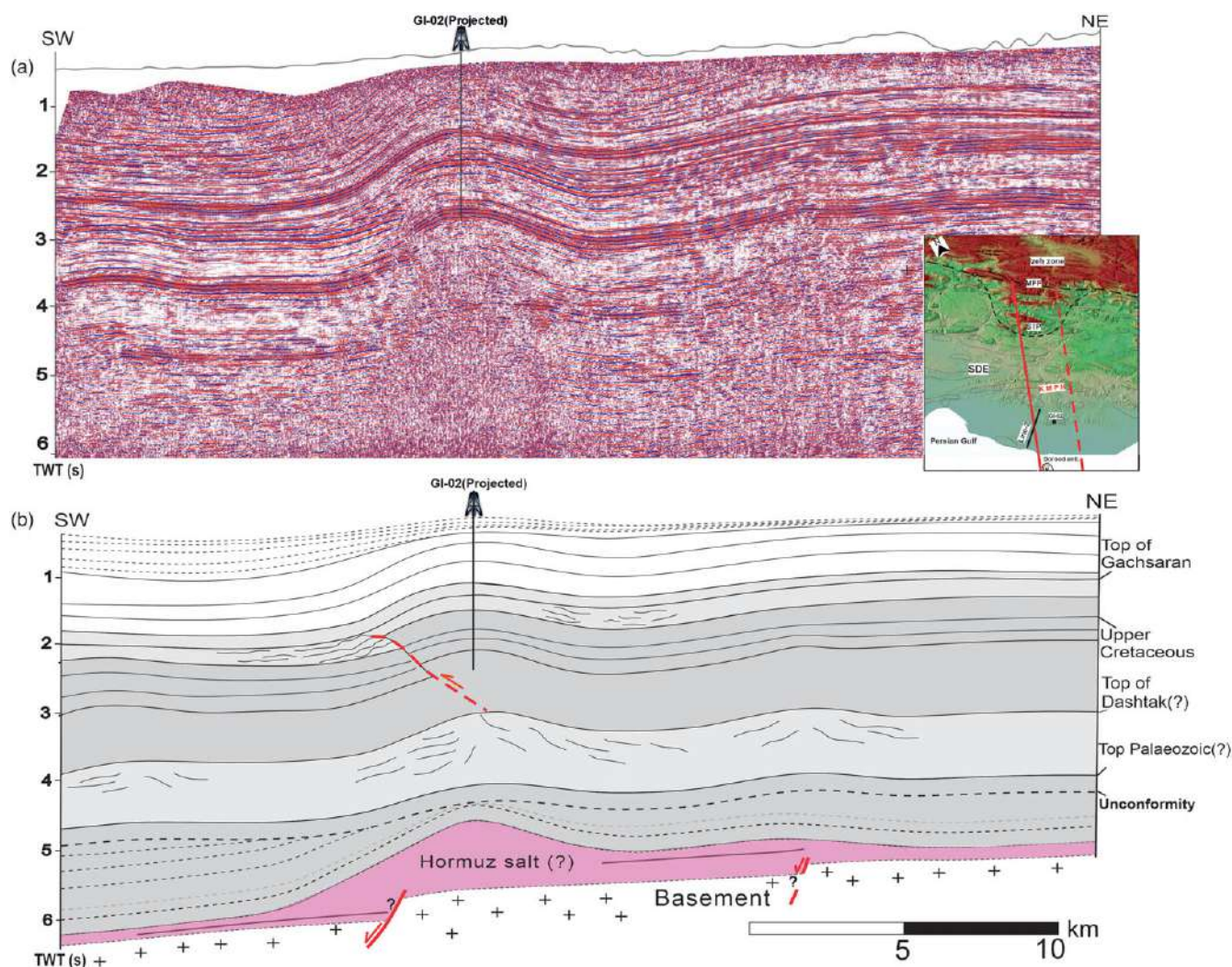
Fig. 6. (Colour online) (a) Uninterpreted and (b) interpreted 2D seismic profile across the KMPH. The seismic line represents a developed deep-rooted anticlinal structure at the western edge of the KMPH (see Fig. 3 for location). Aj-Bk – Aghajari and Bakhtiyari formations; As – Asmari Formation; Bgp – Bangestan Group; D – Doorod well; Gd – Gadvan Formation; Gs – Gachsaran Formation; HD – Hendijan well; Hi – Hith Formation; Kz – Kazhdumi Formation; Mn – Mishan Formation; TWT – two-way travel time.

propagation of the deformation towards the foreland, while in the adjacent zones it continues to propagate as evidenced by the development of two new thrusts (T2-1 and T2-2 in Fig. 12b, c) separated by a relay zone over the structural high.

After 220 mm of shortening, this differential displacement causes a progressive inwards rotation of the structures up to 14° (note the curvature of the passive marker above the structural high in Fig. 12d). Coevally, the anticline growth amplifies until a back-thrust develops in its back-limb oblique to the rest of the structures (Fig. 12d). Further shortening increased tightening of the salt-cored anticline with the development of an imbricate thrust (T2-3) and back-thrust system at the frontal and back limb of this structure, respectively (Figs 12d, 13b). The development of these structures typically indicates the closure of the previous salt anticline and the consequent secondary welding (Fig. 13b). The salt

from the adjacent area feeds the core of these anticlines and the salt is competently depleted. As a result, the central anticline becomes the structure with the highest topographic expression on the model's surface. Shortening has squeezed the salt body welding the back-limb. Here, a foreland-directed thrust-weld nucleates at the pedestal. Thereafter, until 240 mm of shortening, contractional deformation propagates forwards with the development of two new thrusts at each side of the structural high (T3-1 and T3-2; Figs 12d, e, 13a, c). These structures nucleate with different timing from each other, and are located at different sides of the structural high. After 240 cm of shortening, while a foreland-verging thrust (T3-1) characterizes the structure on one side of the structural high, a pop-up structure bounded by a thrust and a back-thrust (T3-2) develops on the other (Figs 12e, 13a,c). Both structures terminate against the structural high, where salt inflates (Fig. 13c). In addition, the salt

Fig. 7. (Colour online) (a) Uninterpreted and (b) interpreted 2D seismic profile of the Golkhari anticline and the western side of the KMPH. Uplift of the NE syncline over the KMPH indicated. The interpreted approximately NE-dipping reverse fault has an associated fold. Gl – Golkhari well (see Fig. 3 for location).

anticline is passively transported over the structural high using the salt layer as a detachment (Fig. 13b). Several extensional faults with a 45° trend develop by crestal collapse of the anticline, indicating coeval squeezing (Fig. 12f).

4.d. Comparison between model and prototype (SIP and SDE)

Lateral and vertical variations in the regional deformation style of the model can be compared with the study area in both the cross-section and map views (Fig. 14). Different along-strike geometry and style of the deformation front could be attributed to the pre-contractional distinct structural features, for example, salt structures (e.g. Davis & Engelder, 1985; Kergaravat et al. 2017) and basement topography (e.g. Molinaro et al. 2004; Razavi Pash et al. 2021b). An underground contour (UGC) map of the top of the Asmari Formation was integrated with the digital elevation model (DEM) to evaluate the key structural elements of the SDE and SIP (Fig. 14b). This map is compared with the interpreted structural features at the end of the experiments on the depth slice (Fig. 14a). The geometry and distribution of the thrust faults concerning the KMPH are visible in the study area and experimental model (Fig. 14). The model indicates thin overburden on top of the

structural high with a pre-contractional salt dome as a weak zone, controlling thrust localization during folding (Letouzey et al. 1995; Letouzey & Sherkati, 2004).

The structural feature in the SDE is comparable between the model and the study area (Fig. 14). The basement high that acted as an indentor controlled the structural gain during shortening by salt inflation and squeezing over the structural high, and by the development of pop-up structures with thrusts and back-thrusts at the adjacent basins. Large-amplitude deflected, tight folds, for example, the Garangan, Chilingar and Gachsaran (eastern nose) anticlines, developed over the KMPH (Fig. 14b). Subsequently, a few large-wavelength folds, for example, the Pazanan, Rag-e-Sefid and Gachsaran (western nose) anticlines developed within the depocenter extended adjacent to the KMPH. Closely spaced and intense brittle structures, such as fore-thrusts, back-thrusts, oblique-slip faults and pop-up structures, more developed over the basement structural high as opposed to the adjacent depocenters (Fig. 14).

Closely spaced thrust faults and high-relief salt-cored anticlines are the main structural features of the SIP. These structures are convergent and then die out towards the two depocenters adjacent
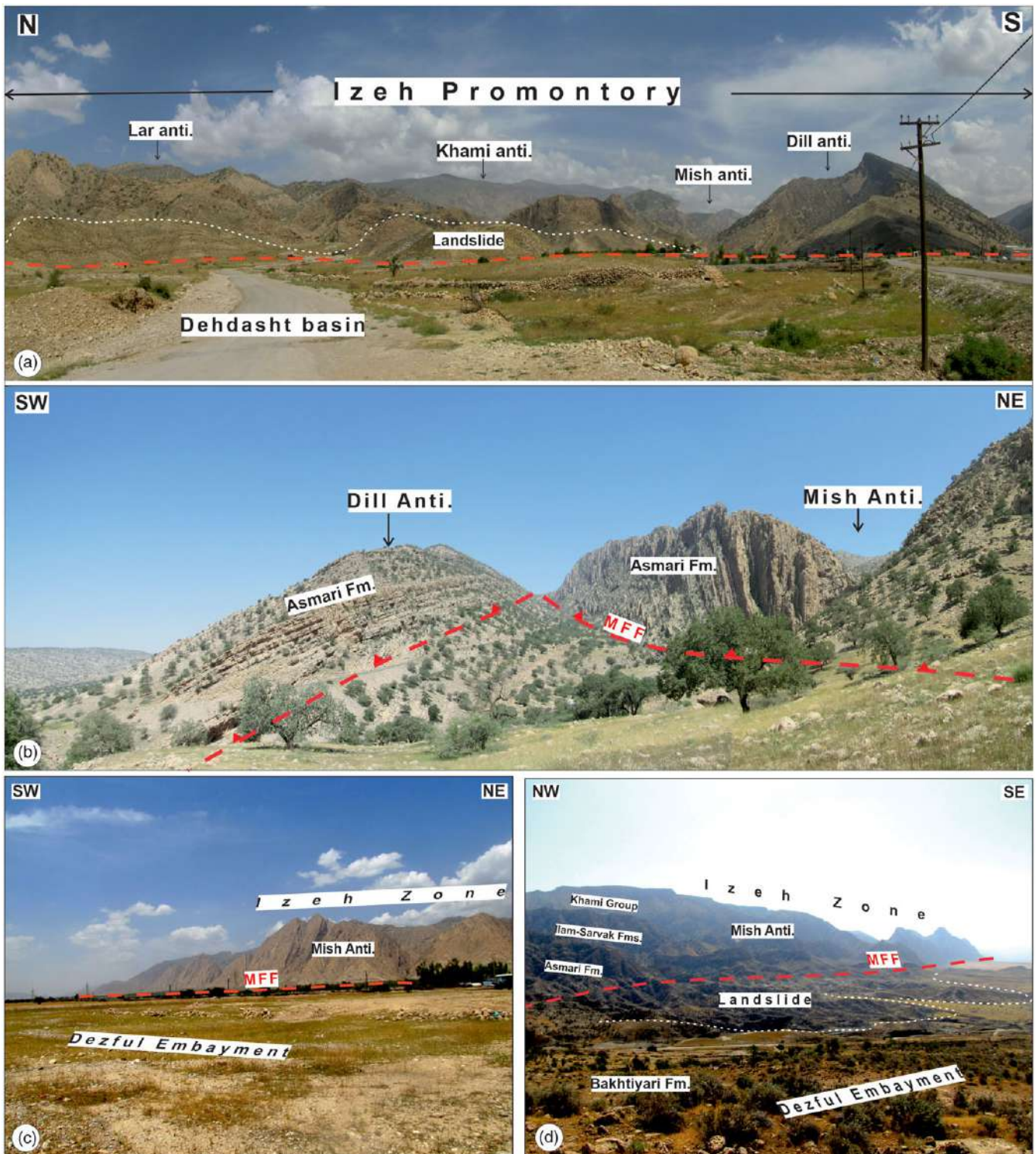
Fig. 8. (Colour online) Landscape photographs of the MFF showing (a) elevation difference between the SIP and Dehdasht basins; (b) emergent SIP thrusts and back-thrusts in the Mish and Dill anticlines; (c) elevation difference between the SIP and Dezful Embayment; and (d) collapse structures and large landslides resulting from the MFF (see Fig. 3 for location).

to the palaeo-high. The Dehdash Basin, a local structural basin in the west of the SIP, is emulated by the model (Fig. 14a). The structural evolution of the Dehdasht Basin specifies a local decrease in the thickness of the Hormuz salt (Heydarzadeh *et al.* 2020). The thick overburden of the Cenozoic sediments in the Dehdasht

Basin can be an effective factor for the withdrawal of basal salt and its movement to the adjacent areas. As simulated in the analogue model, feeding the salt dome over the KMPH by withdrawal from the Dehdasht Basin creates a significant elevation difference between these two areas.
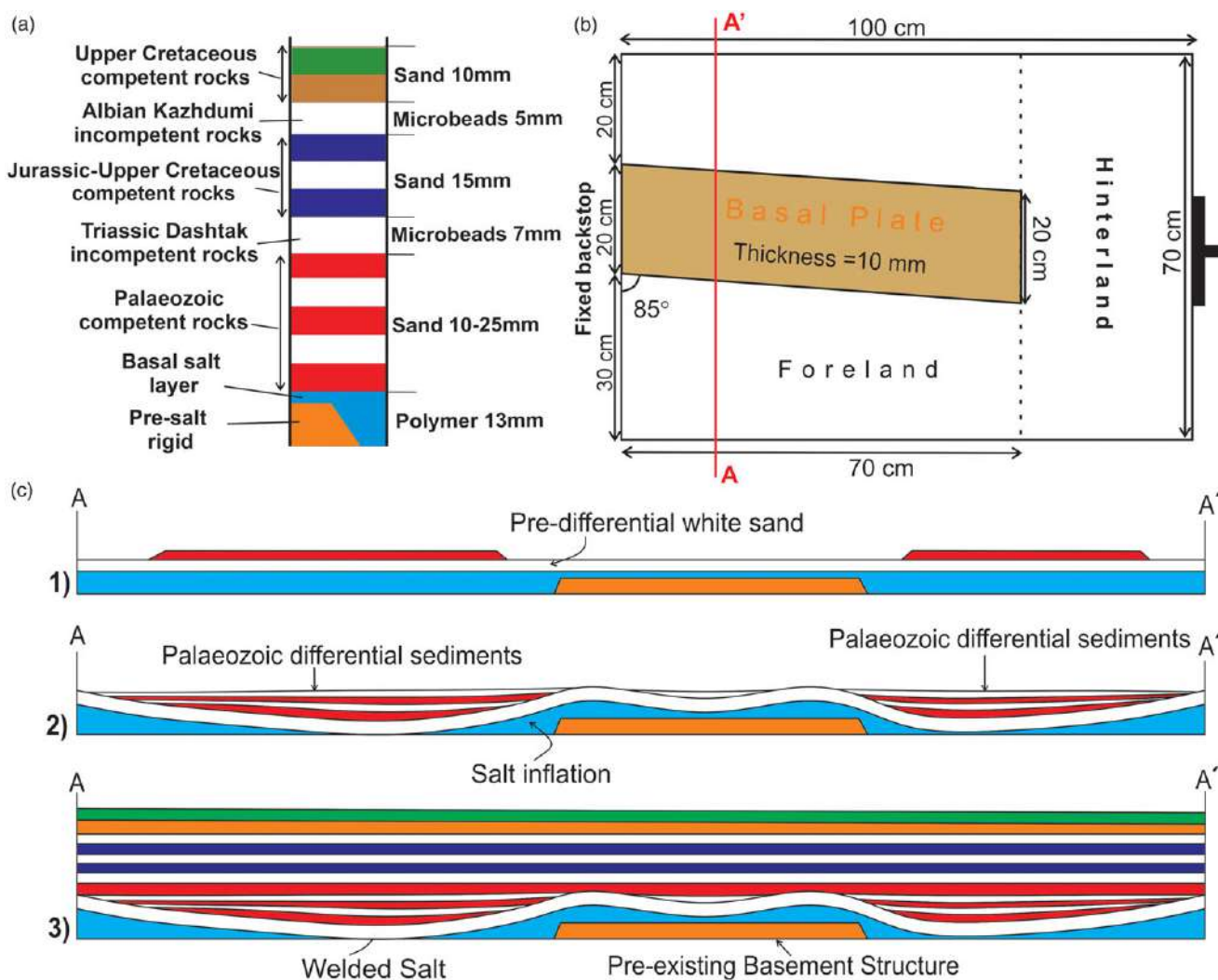
Fig. 9. (Colour online) Experimental set-up. (a) Mechanical properties of the model stratigraphy and equivalent prototype showing the composition of each layer. (b) Schematic top view of apparatus shows the position of the structural high. (c) Pre-contractional evolution of the experiment through conceptual sketches – 1, beginning of the down-building; 2, after salt welding at the end of the down-building stage and 3, at the beginning of the compression.

Some of the SIP structures are still active (e.g. Berberian, 1995; Tavani *et al.* 2020), as characterized by the many earthquakes as well as landslides in this area. This fact is consistent with the results of the experiment that show how the salt-cored anticlines uplifted by squeezing while being transported over the basement high as shortening increased. As contractional deformation progresses and the salt-inflated structure is transported over the structural high, a smooth arc develops. Although this structure is more subtle in our experiment, it is equivalent to the SIP (Fig. 14). Syntectonic sedimentation (not considered in our experiment) or different mechanical properties for the intermediate and upper detachments (Dashtak and Kazhdumi formations) probably enhanced the arcuate geometry of the salient (Pla *et al.* 2019).

5. Discussion

5.a. Evolution of the South Izeh Promontory

Several studies have shown that the reactivation/positive inversion of steeply dipping NW–SE-trending pre-existing basement fault in some parts of the Zagros foreland folded belt (e.g. Mouthereau

et al. 2006; Tavani *et al.* 2020) governed the development of the MFF. However, our study suggests that the SIP, as part of the MFF, developed in relation to the Hormuz salt inflation constrained by inherited pre-salt topography (KMPH) (Fig. 15). The structural development of this study differs from that of Bahroudi & Koyi (2003), in which the variation of basal salt on the deformation style of sedimentary cover was tested without considering the gneissic basement configuration. In addition, Farzipour-Saein *et al.* (2013) demonstrated the effect of the basement step on the propagation of the deformation front during the shortening. Their results demonstrate that the impact of the basal salt in the propagation of the deformation front is greater than that of the thickness variation of the sedimentary cover across the basement step. However, in this work we study the structure and kinematics of the study area based on the detailed structural interpretation aided by previous studies of the area (e.g. Bahroudi & Koyi, 2003; Sherkati *et al.* 2006; Farzipour-Saein *et al.* 2013).

The accumulation of a thick Hormuz salt layer over the KMPH intensified deformation there compared with the adjacent area. The driving mechanism of the Hormuz halokinetic sequences
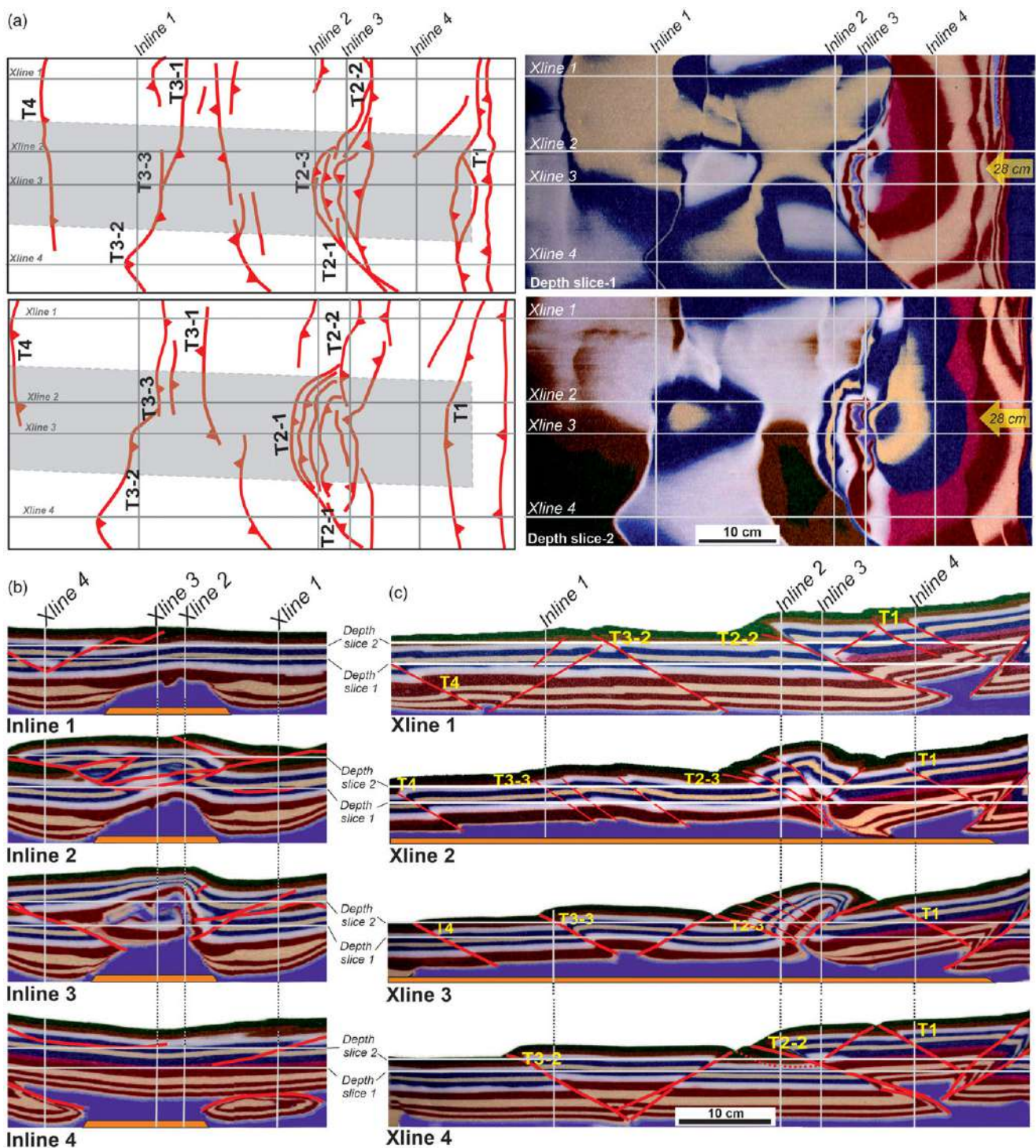
Fig. 10. (Colour online) Different view of developed structures at the end of the shortening – (a) two depth slices at different depths of the model and their respective structural interpretation; (b) four inline sections crossing the structural high (grey rectangle); and (c) four x-line sections along-strike the structural high and depocenters. T1–T4 indicate the main thrusts that developed as shortening increased. The location of each section is highlighted in all figures.

controlled by the KMPH was the squeezing of the pre-contractional salt dome (Fig. 15b) (Letouzey & Sherkati, 2004). The pre-existing structural high significantly weakens the sedimentary cover and localizes the deformation during the shortening, which increases the topography of the structures before the thrusting (Calignano *et al.* 2017; Kergaravat *et al.* 2017; Duffy *et al.* 2018). Thin sedimentary cover over the KMPH contributed greatly to this

deformation style, reducing the mechanical contrast between basal salt and sedimentary cover above the KMPH where deformation can localize. Strain localization by thick salt accumulated over the frontal ramp during the shortening is another reason for the initial rising of basal salt before thrusting.

The overburden at the SIP was arched in response to the active deformation front during shortening. Here, the top of the Asmari
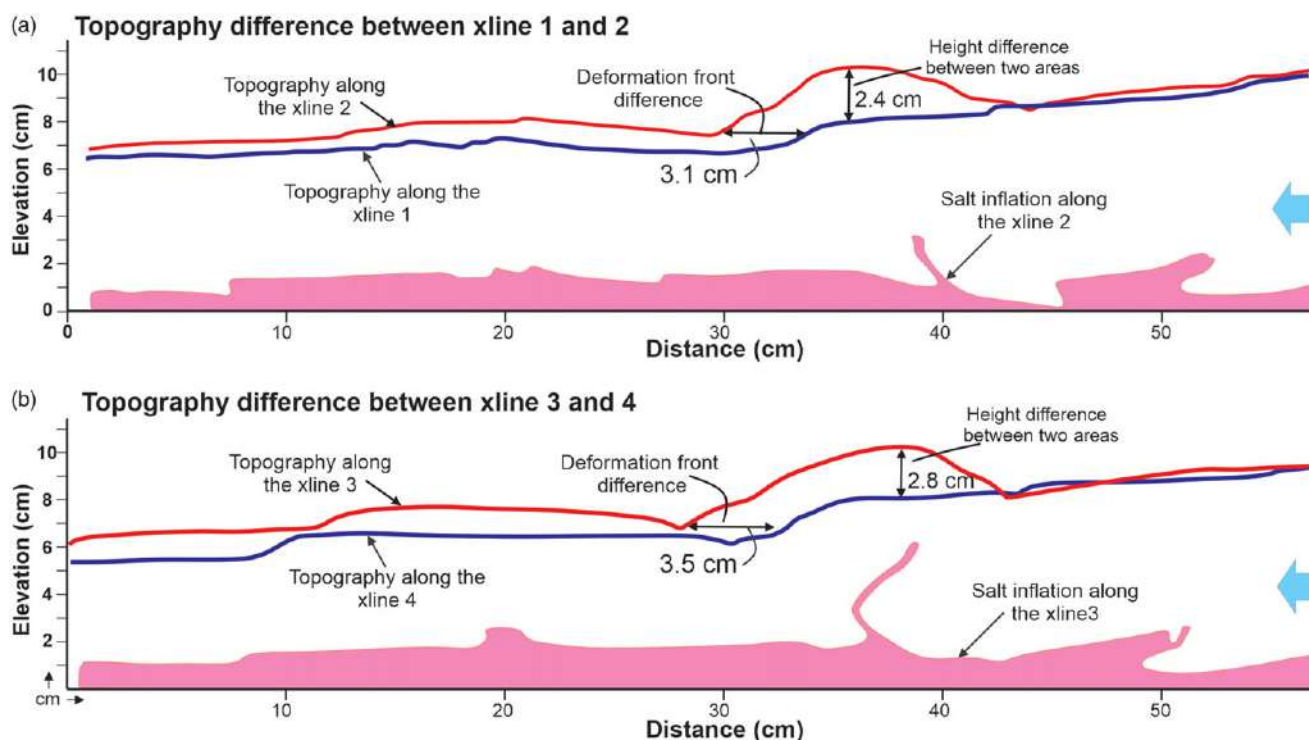
Fig. 11. (Colour online) Topography profile on the surface of the experiment at the end of the shortening shows the different elevation of the structures along the structural high and adjacent depocenters – (a) x-lines 1 and 2; and (b) x-lines 3 and 4. See Figure 10 for the sections. Blue line – along the depocenters; red lines – along the basal plate. The geometry of basal salt along the structural high is highlighted by the pink area in both sections.

Formation is located vertically *c.* 5 km higher than in the SDE (Fig. 14b). This vertical displacement was observed in the field where the Lower Cretaceous sediments of the SIP were placed next to the Plio-Pliostocene sediments of the SDE by several steeply dipping thrusts at the base of the sedimentary cover (Fig. 8). Nevertheless, the thickness of the Hormuz salt at the end downbuilding stage, combined with the presence of the inherited basement high, was critical for the subsequent evolution during the contractional episode (Jahani *et al.* 2017; Snidero *et al.* 2019). The presence of the gneissic basement step below the basal salt localized the deformation in the sedimentary cover. The subsequent shortening resulted in the formation of the ductile ramp above the basement frontal ramp (Bonini *et al.* 2000; Ter Borgh *et al.* 2011). The ductile ramp developed as a result of the presence of a thick salt layer and the buttressing effect of the frontal ramp of KMPH as shortening increases. Salt at the core of the SIP anticlines was fed by the adjacent sinking basins (Heydarzadeh *et al.* 2020) and the hinterland of the structural high.

5.b. Evolution of the Kharg-Mish Palaeo-high

Based on the thickness and facies variations depicted in the well data, several authors concluded that the Kharg-Mish structure acted as a Palaeo-high from early Aptian time (e.g. Motiei, 1994; Farahzadi *et al.* 2019). The effect of the KMPH on the sedimentary cover geometry is depicted via a cross-section based on the well and seismic data in Figure 16, which can be interpreted as a major near-symmetric geometry in the sedimentary cover above the KMPH. Subsidence analyses in the numerous well data of the SDE show that the KMPH is not limited to fault zones, and should be considered as a large-scale structure related to regional up-warping of the basement (Farahzadi *et al.* 2019). The location and geometry of the

KMPH have been geometrically inferred as per the cover deformation patterns characterized by the folding of the lower Palaeozoic reflectors.

The KMPH represents a regional warp of *c.* 40 km width. The section across the KMPH shows an overall asymmetric concave-up geometry caused by extensional faulting of the inherited basement structure, and dominant salt upwarping and inflation as a result of the kinematics of differential ductile salt flow, gliding both laterally and vertically to the central portion of the structure resulting in a dynamic bulge (Fig. 16). The depocenter at the western flank of this structure is dominantly filled by the thick Palaeozoic, Upper Cretaceous and Upper Cenozoic sediments, which gradually thin towards the high. This can be attributed to the reactivation of the basement faults during Phanerozoic time that episodically grew the overlying salt layer (e.g. Letouzey & Sherkati, 2004; Stewart, 2018).

During the Zagros Orogeny, post-Miocene sediments were deposited in the western depocenter to a thickness of > 2 km. Nevertheless, the KMPH is recognizable with a > 2 km height difference from the western depocenters at the top of the Asmari Formation. The anticline geometry of KMPH suggests that the major basement fault zone was decoupled by the Hormuz salt layer from the sedimentary overburden (Fig. 16). Decoupling of sedimentary cover by a salt layer mainly developed close to the edge of the extensional basement fault (Letouzey & Sherkati, 2004).

5.c. Effect of the KMPH on fold style

The subsurface structures across the KMPH in the SDE are characterized by lateral changes in fold style controlled by differences in cover thickness. The thickness and facies variations shown on the stratigraphy column are the main controlling factors on the
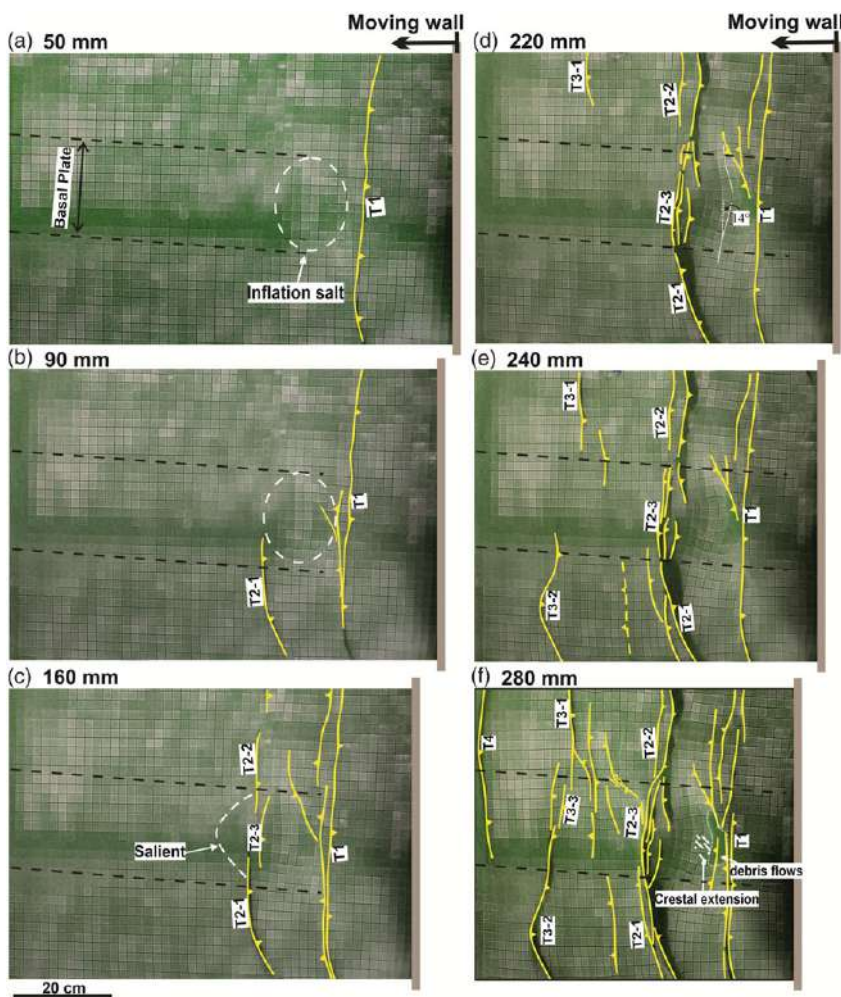
Fig. 12. (Colour online) Overhead photographs showing the kinematic evolution of the experiment after (a) 50 mm; (b) 90 mm; (c) 160 mm; (d) 220 mm; (e) 240 mm; and (f) 280 mm of shortening. T1–T4 indicate the main thrusts that developed as shortening increased. The emergence of the faults at the surface is represented by the yellow lines.

spacing, axial length and wavelength of anticlines (Sherkati & Letouzey, 2004; Sepehr *et al.* 2006; Casciello *et al.* 2009; Motamedi *et al.* 2012; Farzipour-Saein & Koyi 2016). Isopach map and well correlation chart show that the Upper Cretaceous sediments were affected by an important tectonic movement along the KMPH (Figs 4, 5) (Hessami *et al.* 2001b; Sherkati & Letouzey, 2004; Noori *et al.* 2019).

Figure 17 shows significant changes in fold style across two NE–SW-trending seismic reflection profiles along the central part of the KMPH and the western depocenter. The thinner Asmari-Sarvak competent rocks above the KMPH are folded with a small wavelength and possibly detached on top of the Kazhdumi Formation; however, on the western depocenter the folds have a larger wavelength. Several closely spaced steep thrusts and back-thrusts with strike-slip components bounded small folds over the KMPH (Fig. 17a). The initiation of these thrusts is strongly controlled by the pre-contractional salt inflated over the structural high. The geometry of fold in the thick competent layers of the Asmari and Bangestant formations control the overlaying sequences in the Kheirabad structure at the adjacent depocenter (Fig. 17b).

The Kheirabad anticline is bounded by two broad synclines, where they are filled with thick post-Gachsaran sediments of the Mishan, Aghajari and Bakhtiyari formations. Thick sequences of the Aghajari and Bakhtiyari deposits in the Kheirabad anticline have reduced the effect of the material flow of the Gachsaran

evaporites. Consequently, the Gachsaran evaporites do not show significant effects on the overlying Aghajari and Bakhtiyari sediments (Fig. 17b) compared with their effects on the sediments deposited at the top of the KMPH (Fig. 17a). Detached minor folds of the Mishan and Aghajari sediments above the KMPH formed in response to the thick Gachsaran evaporite, which acts as the main décollement. The effect of the Gachsaran evaporates as the main detachment level in the deformation style of the Dezful Embayment structures has already been discussed by several authors (e.g. Letouzey & Sherkati, 2004; Najafi *et al.* 2018). The Kheirabad anticline is a detachment fold with a thrust in its southern forelimb, which probably propagated from the underlying Dashtak evaporites formation. The thin Hormuz salt layer decreases the efficiency as a basal décollement, which activated the intermediate décollement during folding (Motamedi *et al.* 2012). The structure of the Kheirabad anticline is similar in geometry to those developed in the area flanking the structural high of the experiment where the overburden is thicker, imposed by the first down-bulding stage. In contrast, thicker Hormuz salt at the top of the KMPH resulted in a more localized deformation in the overlying sediments.

5.d. Conceptual tectonostratigraphy

We propose a three-step tectonostratigraphic evolution of the KMPH at the SDE and NW of the Persian Gulf based on the results
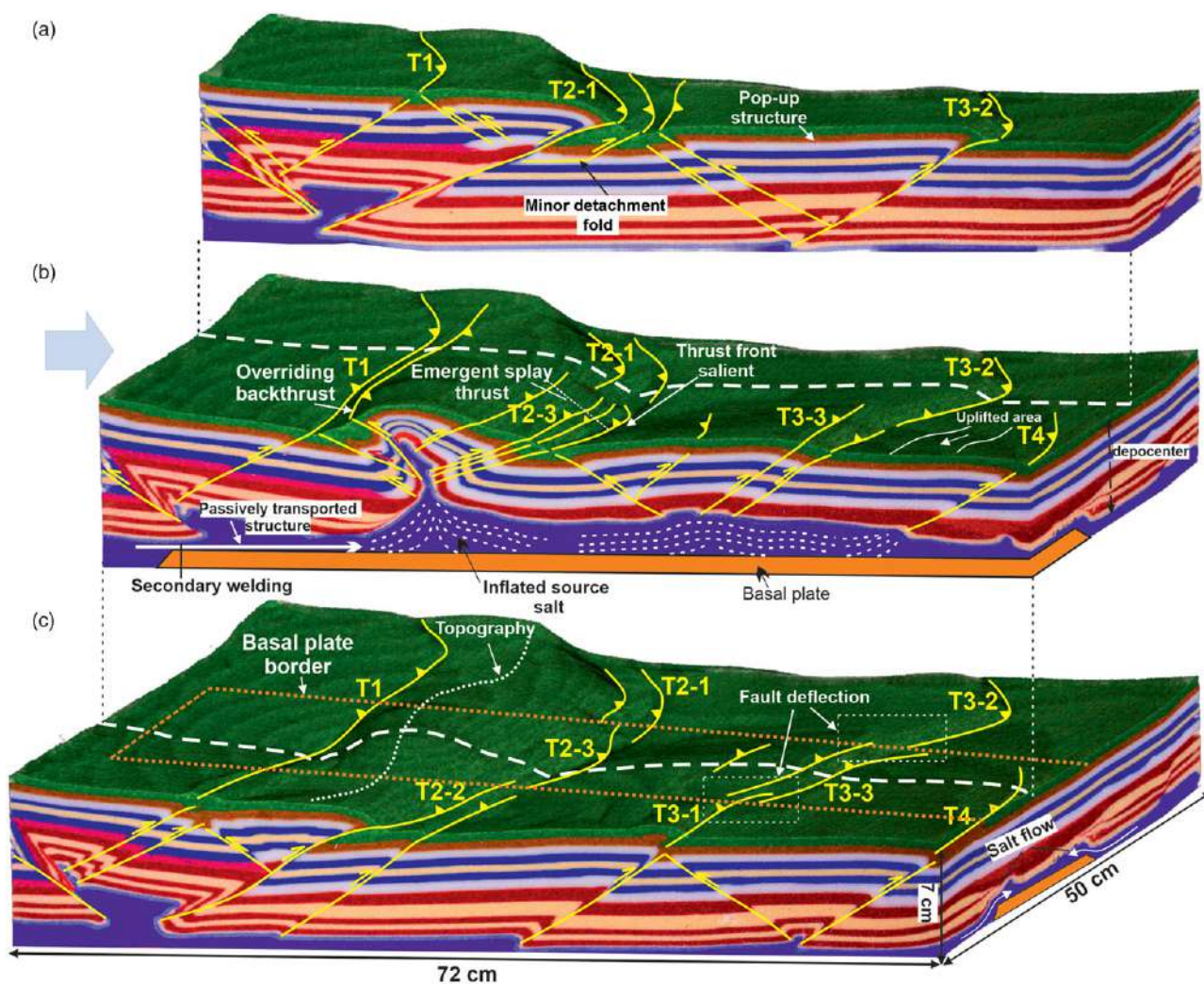
Fig. 13. (Colour online) 3D oblique view of the developed structures at the end of shortening in which interpreted structure traces such as folds and faults are indicated – (a) right-hand side of the basal plate; (b) along with the basal plate; and (c) left-hand side of the basal plate. T1–T4 indicate the main thrusts that developed as shortening increased. The dashed white lines on the surface of (b) and (c) represent the slice location of (a) and (b), respectively.

of this study and previous studies (Fig. 18). Since Late Proterozoic time, various tectonic events have affected the study area.

(1) *Hormuz salt basin during late Proterozoic – early Cambrian time*: the late Proterozoic – Cambrian Hormuz salt basin was controlled by pre-existing horsts and grabens with the sedimentation of evaporites (Fig. 18a; e.g. Alsharhan, 1989; Jahani *et al.* 2017). The horst and graben structures strongly controlled the configuration of the predominantly N–S-trending basement. The N–S-trending KMPH extended towards the SDE. The top-magnetic basement map of the NE Arabian Plate shows the deepening of the basement top from the south towards the north along the KMPH (Morris, 1977; Alavi, 2007; Figs 14b, 18a). However, based on the geometry of the basement it could be considered that the thickness of the Hormuz salt increased towards the hinterland to the NE.

(2) *Basement reactivation by the Carboniferous Hercynian Orogeny*: the reactivation of the deep-rooted extensional faults in the Hercynian Orogeny grew salt structures connected to these basement structures (Faqira *et al.* 2009; Stewart, 2018).

Domal structures NW of the Persian Gulf (e.g. the Dorood field) underwent salt movement linked to the reactivation basement fault (Soleimany *et al.* 2011) (Fig. 18b). This structure is mainly related to the pre-Zagros shortening, and is probably related to the salt flow and basement fault reactivation. It is suggested that the other N–S- to NW–SE-trending oilfields at the top of the KMPH in the SDE witnessed the same tectonic history during Palaeozoic time. Based on the analysis of the subsurface data and structures of the study area, the pre-Hercynian Palaeozoic sediments were most probably eroded over the KMPH during Carboniferous time (Fig. 18b).

(3) *Late Cretaceous – present-day Zagros Orogeny*: after the late Palaeozoic – Early Cretaceous tectonic quiescence, the result of the onset of the Zagros Orogeny, ophiolite obduction in the NE Arabian Plate reactivated pre-existing basement faults (Bahroudi & Talbot, 2003; Sepehr & Cosgrove, 2004, Mohammadrezaei *et al.* 2020; Orang & Gharabeigli, 2020). This is documented by the huge unconformity and growth strata on the Sarvak, Ilam and Gurpi formations. Subsequent shortening caused by the Zagros Orogeny from
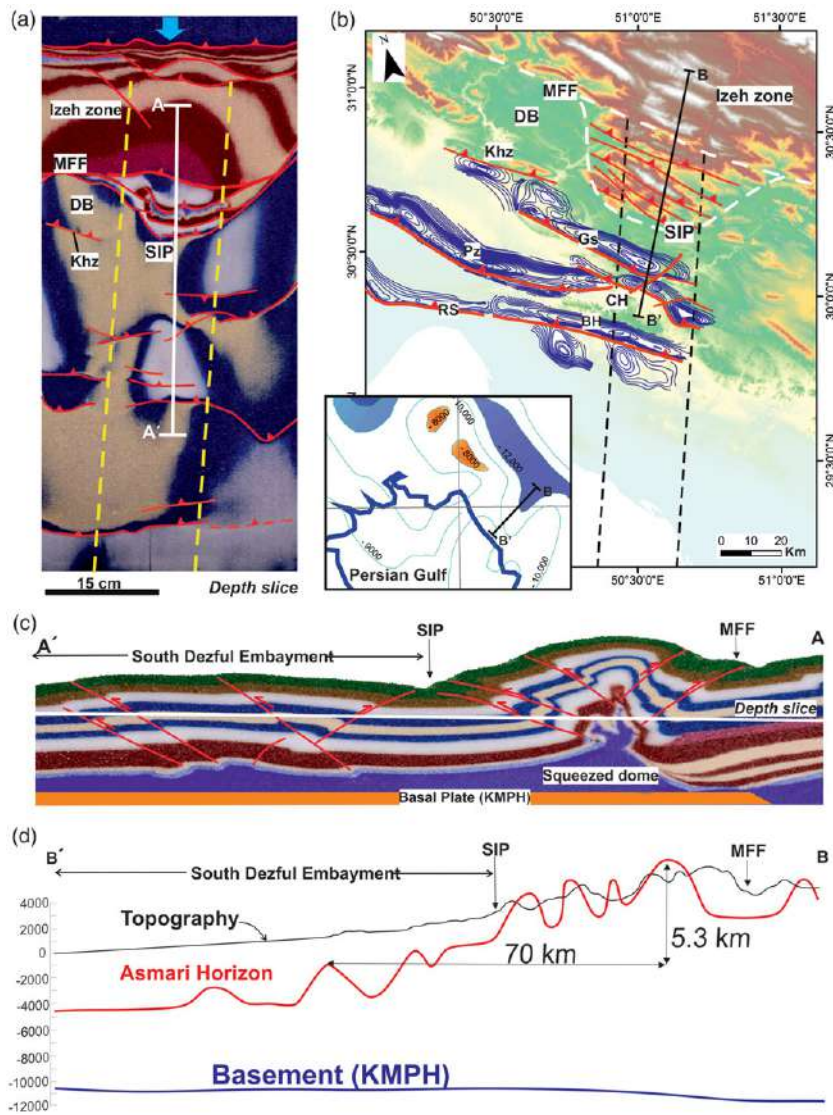
Fig. 14. (Colour online) Overhead and section views of the key structures of the study area. (a) Depth slice of the model at the end of shortening. (b) DEM of the study area overprinted by the UGC map at the top of the Asmari Formation of the SDE structures. The inset map shows the location of the BB′ section on the top-magnetic basement map of the ZFTB (Morris, 1977). (c) 2D section of the model along with the basal plate at the end of the experiment (see (b) for location). (d) Longitudinal profiles for the topography (black) and basement (blue) is based on Morris (1977), and the top of the Asmari Formation (red) in the study area is based on the outcrop and UGC map (see (b) for location). BH – Bibihakimeh anticline; CH – Chilingar anticline; DB – Dehdasht Basin; Gn – Garangan anticline; Gs – Gachsaran anticline; MFF – Mountain Front Flexure; Pz – Pazanan anticline; Rs – Rag-e-Sefid anticline; SIP – South Izeh Promontory.
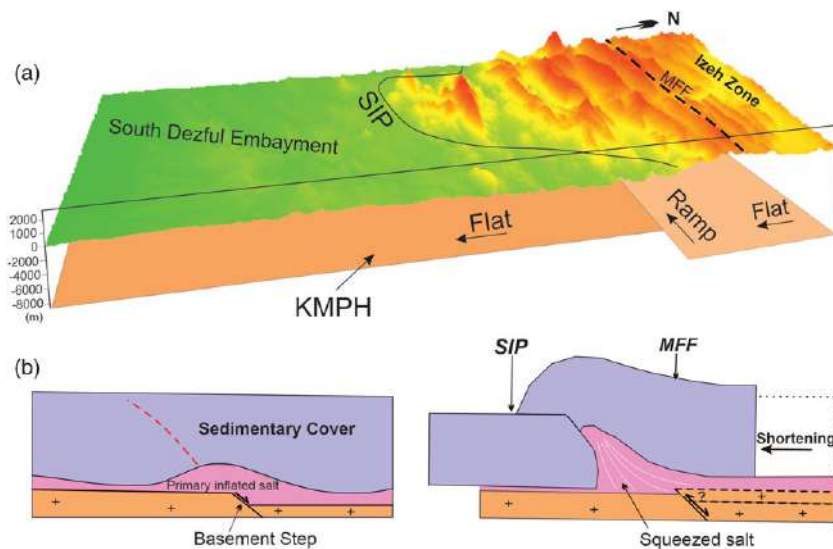
Fig. 15. (Colour online) (a) 3D investigation of surface and basement morphology of the study area on top of the Palaeo-high structure, and interaction between the MFF and the frontal ramp of the KMPH. (b) 2D conceptual cross-sections showing the relation between the frontal ramp of KMPH in association with the salt ductile flow. KMPH – Kharg-Mish Palaeo-high; MFF – Mountain Front Flexure; SIP – South Izeh Promontory.
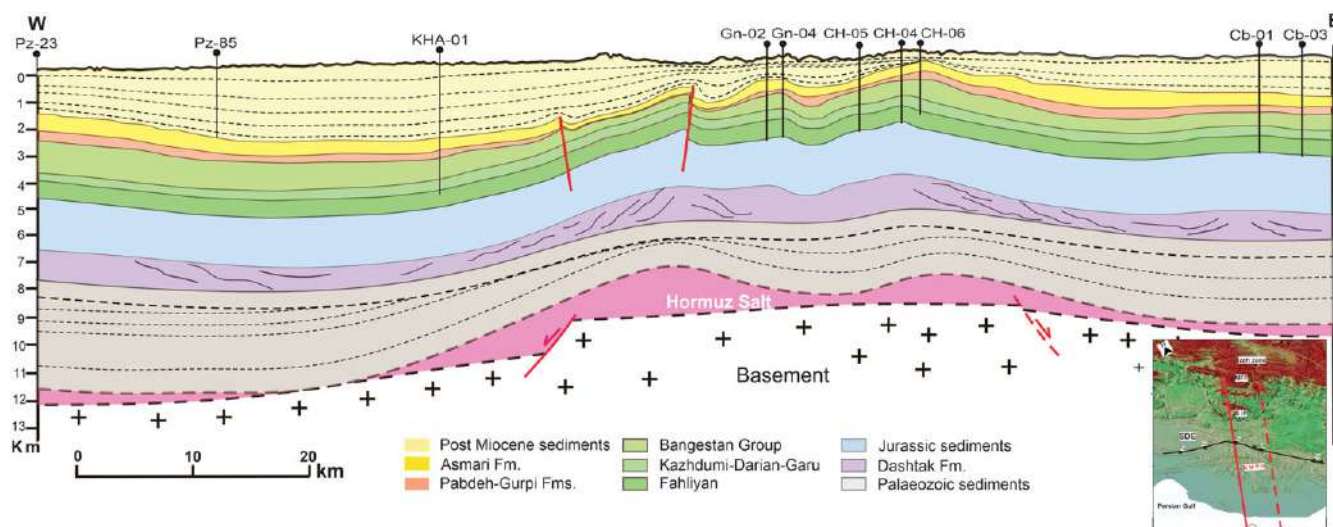
Fig. 16. (Colour online) An interpreted longitudinal section through Pazanan, Kheirabad, Garangan, Chilingar and Chahar-Bisheh fields, perpendicular to KMPH, based on the well and seismic data. Cb – Chaharbisheh well; CH – Chilingar well; Gn – Garangan well; KHA – Kheirabad well; Pz – Pazanan well.
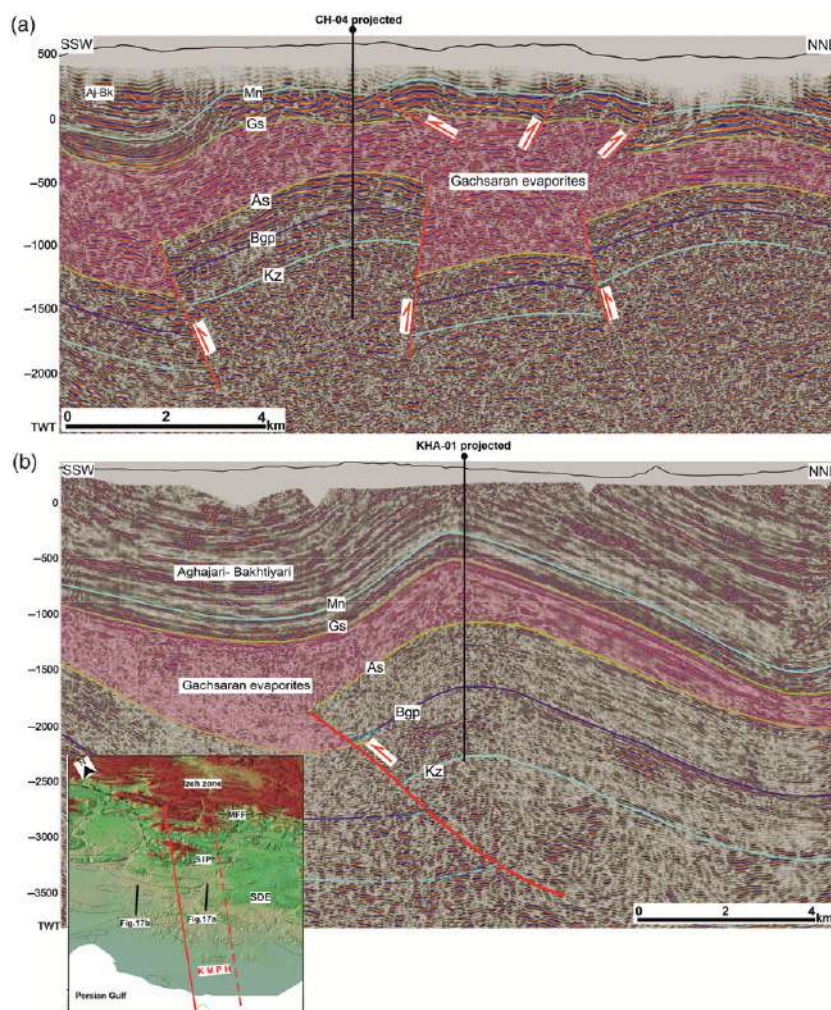
Fig. 17. (Colour online) Interpreted 2D seismic sections of the structures in the SDE. (a) Line-1 – structures on top of the KMPH; and (b) Line-2 – Kheirabad anticline in the western depocenters of the KMPH (see Fig. 3 for location). Aj-Bk – Aghajari-Bakhtiyari Fms; As – Asmari Formation; Bgp – Bangestan Group; Gs – Gachsaran Formation; Kz – Kazhdumi Fm; Mn – Mishan Formation.

Late Cretaceous time until the present day resulted in a thin-skinned deformation that detached over the basal salt in the SDE. It was then converted to a thick-skinned deformation in a process involving the pre-existing basement structures (Fig. 18c). The pre-existing Dorood structure, located far from the hinterland part and towards the foreland, demonstrates deformation by the Zagros shortening processes.
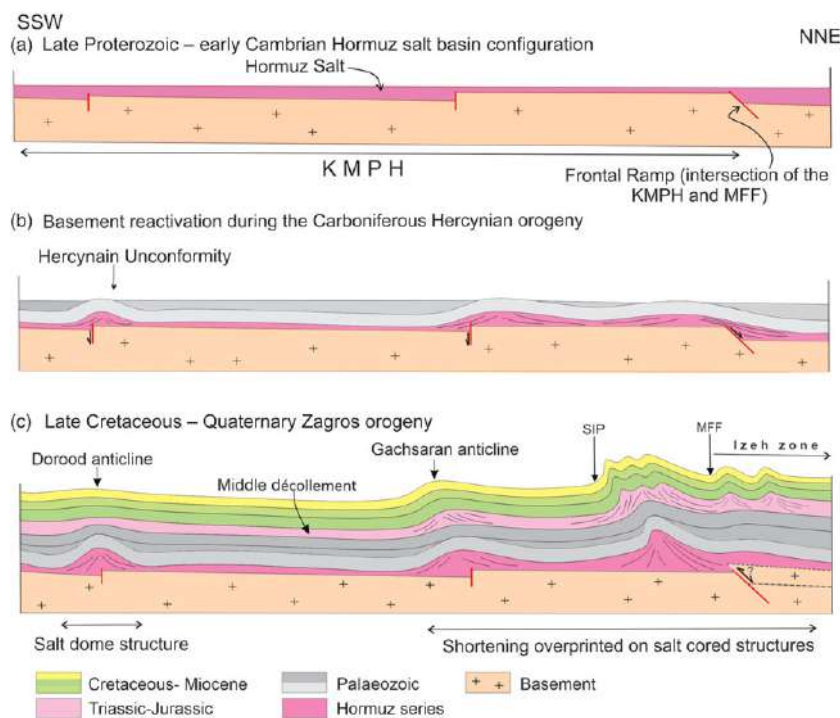
Fig. 18. (Colour online) 2D conceptual kinematic evolution from MFF to the coastline of the Persian Gulf (not to scale). The section was constructed along the KMPH. See Figure 1 for the location of the Dorood (D) and Gachsaran (Gs) anticlines.

Although we have mostly focused on the role of the N–S-trending basement structure on the structural evolution, the important role of the NW–SE-trending basement faults should not be neglected in considering the structural evolution of the area (Sherkati & Letouzey, 2004). The intersection of these two basement trends, which was addressed in this study, better shows the role of the basement configuration in the structural evolution of the area. Nevertheless, the basement structures below the salt layer act weakly, which could nucleate deformation during the extensional, contractional or passive downbuilding processes. In the SIP, at the intersection of the KMPH and MFF, ductile flow over the basement structures as a result of contraction of the Hormuz salt led to the salt-cored anticlines of the SIP. This augmented salt flow over the frontal ramp of the KMPH (Fig. 18c).

Although this study has mainly considered the effect of the basal décollement on the structural style of the sedimentary cover, several researchers have also addressed the impact of the intermediate décollement layers on the fold style during the contractional deformation of the Zagros Orogeny (Fig. 18c; e.g. Sherkati & Letouzey, 2004; Derikvand *et al.* 2018).

5.e. Implications for hydrocarbon exploration

In the NE Arabian Plate, the N–S-elongated oilfields along the pre-existing basement faults rotated to NW–SE-aligned trends due to the overprinting of the Zagros shortening (Talbot & Alavi, 1996; Hessami *et al.* 2001*b*; Mohammadrezaei *et al.* 2020). This fact is documented by the pattern of the oilfields in the NW of the Persian Gulf and SDE along with the Kharg-Mish and Hendijan-Bahregansar palaeo-highs (Fig. 1). In addition, the oilfields structure in the SDE varies significantly in size and style because of the different kinematic evolution across the KMPH. The well-known middle Cretaceous – early Miocene petroleum system in the Dezful Embayment is separated from two older systems (Palaeozoic and Jurassic) by thick evaporate sediments

(Bordenave & Hegre, 2005). The Upper Cretaceous Bangestan reservoir, the second main reservoir in the SDE, is significantly affected by the KMPH reactivation. During the Late Cretaceous uplift, the Bangestan reservoir was eroded and the reservoir quality was enhanced by fractures and fault systems at the top of the KMPH. It is suggested that the development of the fractures was related to the reactivation of the basement fault in the Dezful Embayment, possibly enhancing the porosity and permeability of the reservoir rock (McQuillan, 1985, 1991; Ahmadhadi *et al.* 2007). Furthermore, the timing of folding during the shortening of the SDE was strongly affected by the presence of the KMPH (as explained in the experimental results), which is important in terms of hydrocarbon migration. The anticlines that formed earlier may be favoured locations for hydrocarbon entrapment. In addition, the style of the individual fields is controlled by the stratigraphy, the structural architecture and the depth to the basement of the basin. However, reservoir, source and cap rocks in the SDE are controlled by the repeated reactivation of the KMPH.

6. Conclusions

This study characterized the different structural styles of the SDE in response to the pre-contractional KMPH using integrated field-based observation, subsurface data and analogue modelling. According to interpreted subsurface data, the reactivation of the KMPH during Phanerozoic time that episodically grew the overlying salt layer resulted in the gradual thinning of the Palaeozoic, Upper Cretaceous and upper Cenozoic sediments from the adjacent depocenters towards the high.

Fold style varies both laterally and vertically in the sedimentary cover as a result of the basal décollement layer and thickness variations of the sedimentary cover. Generally, fold structures in the SDE appear in large wavelengths in the depocenters where the sedimentary cover is thick, while small-wavelength and disharmonic folds developed over the KMPH.

Supporting experimental results, the pre-existing basement structure and overlying salt layer are critical controlling factors on strain localization, deformation pattern, fold style, spatial and temporal nucleation and propagation of structures, and the structural evolution of the salt-influenced fold-and-thrust belt. In other words, induced heterogeneities between the basement and overlaid salt layer are a controlling factor in the deformation of the sedimentary cover during the subsequent thin-skinned shortening.

The modelling results demonstrate that the intersection between the frontal ramp of the KMPH and MFF acts as a ductile ramp and a passive indentor during the shortening process. As shortening progresses to the foreland, strain localization and amplification over the ductile ramp of the KMPH are accommodated by a rising SIP, which is much higher than the two surrounding basins. Closely spaced thrust faults and high-relief salt-cored anticlines are the main structural features of the SIP.

The results of this study indicate that the basal architecture of the sedimentary basin, which is influenced by the basement structures and the salt layers, is one of the most important factors in the nucleation, style and evolution of structures, and their relative timing. These factors will have a far-reaching implication in future hydrocarbon exploration in the study area.

References

Abdullahie Fard I, Braathen A, Mokhtari M and Alavi SA (2006) Interaction of the Zagros fold–thrust belt and the Arabian-type, deep-seated folds in the Abadan Plain and the Dezful Embayment, SW Iran. *Petroleum Geoscience* **12**, 347–62.

Abdullahie Fard I, Sepehr M and Sherkati S (2011) Neogene salt in SW Iran and its interaction with Zagros folding. *Geological Magazine* **148**, 854–67.

Ahmadhadi F, Lacombe O and Daniel JM (2007) Early reactivation of basement faults in Central Zagros (SW Iran): evidence from pre-folding fracture populations in Asmari Formation and lower Tertiary paleogeography. In *Thrust Belts and Foreland Basins: From Fold Kinematics to Hydrocarbon Systems* (eds O Lacombe, F Roure, J Lavé and J Vergés), pp. 205–28. Berlin, Heidelberg: Springer.

Al-Husseini MI (2000) Origin of the Arabian plate structures: Amar collision and Najd rift. *GeoArabia* **5**, 527–42.

Alavi M (1994) Tectonics of the Zagros orogenic belt of Iran: new data and interpretations. *Tectonophysics* **229**, 211–38.

Alavi M (2004) Regional stratigraphy of the Zagros fold-thrust belt of Iran and its pro-foreland evolution. *American Journal of Science* **304**, 1–20.

Alavi M (2007) Structures of the Zagros fold-thrust belt in Iran. *American Journal of Science* **307**, 1064–95.

Allen MB and Talebian M (2011) Structural variation along the Zagros and the nature of the Dezful Embayment. *Geological Magazine* **148**, 911–24.

Alsharhan AS (1989) Petroleum geology of the United Arab Emirates. *Journal of Petroleum Geology* **12**, 253–88.

Asgari G, Ghaemi F, Soleimany B, Rahimi B and Maleki M (2019) Determine folding mechanism of Lali structure, northern Dezful, Zagros, Iran. *Iranian Journal of Earth Sciences* **11**, 113–25.

Asl ME, Faghih A, Mukherjee S and Soleimany B (2019) Style and timing of salt movement in the Persian Gulf basin, offshore Iran: insights from halo-kinetic sequences adjacent to the Tonb-e-Bozorg salt diapir. *Journal of Structural Geology* **122**, 116–32.

Bahroudi A and Koyi HA (2003) Effect of spatial distribution of Hormuz salt on deformation style in the Zagros fold-and-thrust belt: an analogue modelling approach. *Journal of the Geological Society* **160**, 719–33.

Bahroudi A and Talbot CJ (2003) The configuration of the basement beneath the Zagros Basin. *Journal of Petroleum Geology* **26**, 257–82.

Berberian M (1995) Master "blind" thrust faults hidden under the Zagros folds: active basement tectonics and surface tectonics surface morphotectonics. *Tectonophysics* **241**, 193–224.

Berberian M and King GCP (1981) Towards a paleogeography and tectonic evolution of Iran. *Canadian Journal of Earth Sciences* **18**, 210–65.

Bonini M, Sokoutis D, Mulugeta G and Katrivanos E (2000) Modelling hanging wall accommodation above rigid thrust ramps. *Journal of Structural Geology* **22**, 1165–79.

Bordenave ML and Hegre JA (2005) The influence of tectonics on the entrapment of oil in the Dezful Embayment, Zagros Foldbelt, Iran. *Journal of Petroleum Geology* **28**, 339–68.

Bordenave ML and Hegre JA (2010) The current distribution of oil and gas fields in the Zagros Fold Belt of Iran and contiguous offshore as the result of the petroleum systems. In *Tectonic and Stratigraphic Evolution of Zagros and Makran during the Mesozoic–Cenozoic* (eds P Leturmy and C Robin), pp. 291–353. Geological Society of London, Special Publication no. 330.

Borderie S, Vendeville BC, Graveleau F, Witt C, Dubois P, Baby P and Calderon Y (2019) Analogue modeling of large-transport thrust faults in evaporites-floored basins: example of the Chazuta Thrust in the Huallaga Basin, Peru. *Journal of Structural Geology* **123**, 1–17.

Burberry CM and Swiatlowski JL (2016) Evolution of a fold-thrust belt deforming a unit with pre-existing linear asperities: insights from analog models. *Journal of Structural Geology* **87**, 1–18.

Caër T, Souloumiac P, Maillot B, Leturmy P and Nussbaum C (2018) Propagation of a fold-and-thrust belt over a basement graben. *Journal of Structural Geology* **115**, 121–31.

Calignano E, Sokoutis D, Willingshofer E, Brun JP, Gueydan F and Cloetingh S (2017) Oblique contractional reactivation of inherited heterogeneities: cause for arcuate orogens. *Tectonics* **36**, 542–58.

Callot JP, Trocmé V, Letouzey J, Albouy E, Jahani S and Sherkati S (2012) Pre-existing salt structures and the folding of the Zagros mountains. In *Salt Tectonics, Sediments and Prospectivity* (eds GI Alsop, SG Archer, AJ Hartley, NT Grant and R Hodgkinson), pp. 545–61. Geological Society of London, Special Publication no. 363.

Carruba S, Perotti CR, Buonaguro R, Calabrò R, Carpi R and Naini M (2006) The structural pattern of the Zagros fold-and-thrust belt in the Dezful Embayment (SW Iran). *Geological Society of America Special Papers* **414**, 11.

Casciello E, Vergés J, Saura E, Casini G, Fernández N, Blanc E and Hunt DW (2009) Fold patterns and multilayer rheology of the Lurestan Province, Zagros simply folded belt (Iran). *Journal of the Geological Society of London* **166**(5), 947 –59.

Colman-Sadd SP (1978) Fold development in Zagros simply folded belt, Southwest Iran. *AAPG Bulletin* **62**, 984–1003.

Cotton JT and Koyi HA (2000) Modelling of thrust fronts above ductile and frictional detachments: application to structures in the Salt Range and Potwar Plateau, Pakistan. *Geological Society of America Bulletin* **112**, 351–63.

Davis DM and Engelder T (1985) The role of salt in fold-and-thrust belts. *Tectonophysics* **119**, 67–88.

Dell'Ertole D and Schellart WP (2013) The development of sheath folds in viscously stratified materials in simple shear conditions: an analogue approach. *Journal of Structural Geology* **56**, 129–41.

Derikvand B, Alavi SA, Abdullahie Fard I and Hajialibeigi H (2018) Folding style of the Dezful Embayment of Zagros Belt: signatures of detachment horizons, deep-rooted faulting, and syn-deformation deposition. *Marine and Petroleum Geology* **91**, 501–18.

Dooley TP and Hudec MR (2020) Extension and inversion of salt-bearing rift systems. *Solid Earth* **11**, 1187–204.

Dooley T, McClay K R, Hempton M and Smit D (2005) Salt tectonics above complex basement extensional fault systems: results from analogue modelling. In *Petroleum Geology: North-West Europe and Global Perspectives – Proceedings of the 6th Petroleum Geology Conference* (eds AG Doré and BA Vining), pp. 1631–48. Geological Society of London, Petroleum Geology Conference Series no. 6.

Duffy OB, Dooley TP, Hudec MR, Jackson MP, Fernandez N, Jackson CA and Soto JI (2018) Structural evolution of salt-influenced fold-and-thrust belts: a synthesis and new insights from basins containing isolated salt diapirs. *Journal of Structural Geology* **114**, 206–21.

Edgell HS (1991) Proterozoic salt basins of the Persian Gulf area and their role in hydrocarbon generation. *Precambrian Research* **54**, 1–14.

Edgell HS (1992) Basement tectonics of Saudi Arabia as related to oil field structures. In *Basement Tectonics 9. Proceedings of the International Conferences on Basement Tectonics, vol. 3* (eds MJ Rickard, HJ Harrington and PR Williams), pp. 169–93. Dordrecht: Springer.

Edgell HS (1996) Salt tectonism in the Persian Gulf basin. In *Salt Tectonics* (eds GI Alsop, DJ Blundell and I Davison), pp. 129–51. Geological Society of London, Special Publication no. 100.

Espurt N, Wattellier F, Philip J, Hippolyte JC, Bellier O and Bestani L (2019) Mesozoic halokinesis and basement inheritance in the eastern Provence fold-thrust belt, SE France. *Tectonophysics* **766**, 60–80.

Falcon NL (1974) Southern Iran: Zagros mountains. In *Mesozoic–Cenozoic Orogenic Belts: Data for Orogenic Studies* (ed. AM Spencer), pp. 199–211. Geological Society of London, Special Publication no. 4.

Faqira M, Rademakers M and Afifi AM (2009) New insights into the Hercynian Orogeny, and their implications for the Paleozoic Hydrocarbon System in the Arabian plate. *GeoArabia* **14**, 199–228.

Farahzadi E, Alavi SA, Sherkati S and Ghassemi MR (2019) Variation of subsidence in the Dezful Embayment, SW Iran: influence of reactivated basement structures. *Arabian Journal of Geosciences* **12**, 616.

Farzipour-Saein A and Koyi H (2016) Intermediate décollement activation in response to the basal friction variation and its effect on folding style in the Zagros fold-thrust belt, an analogue modelling approach. *Tectonophysics* **68**, 56–65.

Farzipour-Saein A, Nilfouroushan F and Koyi H (2013) The effect of basement step/topography on the geometry of the Zagros fold-and-thrust belt (SW Iran): an analog modelling approach. *International Journal of Earth Sciences* **102**, 2117–35.

Farzipour-Saein A, Yassaghi A, Sherkati S and Koyi H (2009) Basin evolution of the Lurestan region in the Zagros fold-and-thrust belt, Iran. *Journal of Petroleum Geology* **32**, 5–19.

Ferrer O, Jackson MP, Roca E and Rubinat M (2012) Evolution of salt structures during extension and inversion of the Offshore Parentis Basin (Eastern Bay of Biscay). In *Salt Tectonics, Sediments and Prospectivity* (eds GI Alsop, SG Archer, AJ Hartley, NT Grant and R Hodgkinson), pp. 361–80. Geological Society of London, Special Publication no. 363.

Ferrer O, Roca E and Vendeville BC (2014) The role of salt layers in the hangingwall deformation of kinked-planar extensional faults: insights from 3D analogue models and comparison with the Parentis Basin. *Tectonophysics* **636**, 338–50.

Godin L, Roche RS, Waffle L and Harris LB (2019) Influence of inherited Indian basement faults on the evolution of the Himalayan orogen. In *Crustal Architecture and Evolution of the Himalaya–Karakoram–Tibet Orogen* (eds R Sharma, IM Villa and S Kumar), pp. 251–76. Geological Society Special Publication no. 481.

Granado P, Ferrer O, Muñoz JA, Thöny W and Strauss P (2017) Basin inversion in tectonic wedges: insights from analogue modelling and the Alpine-Carpathian fold-and-thrust belt. *Tectonophysics* **703**, 50–68.

Hassaan M, Faleide JI, Gabrielsen RH, Tsikalas F and Grimstad S (2021) Interplay between base-salt relief, progradational sediment loading and salt tectonics in the Nordkapp Basin, Barents Sea–Part II. *Basin Research* **33**(6), 3256–94.

Hessami K, Koyi HA and Talbot CJ (2001a) The significance of strike-slip faulting in the basement of the Zagros fold-and-thrust belt. *Journal of Petroleum Geology* **24**, 5–28.

Hessami K, Koyi HA, Talbot CJ, Tabasi H and Shabanian E (2001b) Progressive unconformities within an evolving foreland fold–thrust belt, Zagros mountains. *Journal of the Geological Society* **158**, 969–81.

Hessami K, Nilforoushan F and Talbot CJ (2006) Active deformation within the Zagros Mountains deduced from GPS measurements. *Journal of the Geological Society* **163**, 143–48.

Heydarzadeh K, Ruh JB, Vergés J, Hajialibeigi H and Gharabeigli G (2020) Evolution of a structural basin: numerical modelling applied to the Dehdasht Basin, Central Zagros, Iran. *Journal of Asian Earth Sciences* **187**, 104088.

Hinsch R and Bretis B (2015) A semi-balanced section in the northwestern Zagros region: constraining the structural architecture of the Mountain Front Flexure in the Kirkuk Embayment, Iraq. *GeoArabia* **20**, 41–62.

Homke S, Vergés J, Garcés M, Emami H and Karpuz R (2004) Magnetostratigraphy of Miocene–Pliocene Zagros foreland deposits in the front of the Push-e Kush arc (Lurestan Province, Iran). *Earth and Planetary Science Letters* **225**, 397–410.

Hubbert MK (1937) Theory of scale models as applied to the study of geologic structures. *Bulletin of the Geological Society of America* **48**, 1459–520.

Husseini MI (1988) The Arabian infracambrian extensional system. *Tectonophysics* **148**, 93–103.

Husseini MI (1989) Tectonic and deposition model of late Precambrian-Cambrian Arabian and adjoining plates. *AAPG Bulletin* **73**, 1117–31.

Jahani S, Hassanpour J, Mohammadi-Firouz S, Letouzey J, de Lamotte DF, Alavi SA and Soleimany B (2017) Salt tectonics and tear faulting in the central part of the Zagros Fold-thrust Belt, Iran. *Marine and Petroleum Geology* **86**, 426–46.

Jassim SZ and Goff JC (eds) (2006) *Geology of Iraq*. Prague: DOLIN. sro, distributed by Geological Society of London.

Karasözen E, Nissen E, Bergman EA and Ghods A (2019) Seismotectonics of the Zagros (Iran) from orogen-wide, calibrated earthquake relocations. *Journal of Geophysical Research: Solid Earth* **124**, 9109–29.

Kent PE (1979) The emergent Hormuz salt plugs of southern Iran. *Journal of Petroleum Geology* **2**, 117–144.

Kergaravat C, Ribes C, Callot JP and Ringenbach JC (2017) Tectono-stratigraphic evolution of salt-controlled minibasins in a fold-and-thrust belt, the Oligo-Miocene central Sivas Basin. *Journal of Structural Geology* **102**, 75–97.

Konert G, Afifi AM, Al-Hajri SA, de Groot K, Al Naim AA and Droste HJ (1999) Paleozoic stratigraphy and hydrocarbon habitat of the Arabian plate. *AAPG Bulletin* **83**, 1320–36.

Koop WJ and Stoneley R (1982) Subsidence history of the Middle East Zagros basin, Permian to recent. *Philosophical Transactions of the Royal Society, London, Series A* **305**, 149168.

Koyi H, Jenyon MK and Petersen K (1993) The effect of basement faulting on diapirism. *Journal of Petroleum Geology* **16**, 285–312.

Koyi HA and Maillot B (2007) Tectonic thickening of hanging-wall units over a ramp. *Journal of Structural Geology* **29**, 924–32.

Koyi HA and Vendeville BC (2003) The effect of décollement dip on geometry and kinematics of model accretionary wedges. *Journal of Structural Geology* **25**, 1445–50.

Lacombe O and Bellahsen N (2016) Thick-skinned tectonics and basement-involved fold–thrust belts: insights from selected Cenozoic orogens. *Geological Magazine* **153**, 763–810.

Letouzey J, Colletta B, Vially RA and Chermette JC (1995) Evolution of salt-related structures in compressional settings. In *Salt Tectonics: A Global Prospective* (eds MPA Jackson, DG Roberts and S Snelson), pp. 41–60. Tulsa: AAPG, Memoir no. 65.

Letouzey J and Sherkati S (2004) Salt movement, tectonic events, and structural style in the central Zagros fold-and-thrust belt (Iran). In *Salt-Sediment Interactions and Hydrocarbon Prospectivity, 24th Annual Research Conference*, Gulf Coast Section, SEPM Foundation, pp. 444–63.

McQuarrie N (2004) Crustal scale geometry of the Zagros fold-thrust belt, Iran. *Journal of Structural Geology* **26**, 519–35.

McQuillan H (1985) Fracture-controlled production from the Oligo-Miocene Asmari Formation in Gachsaran and Bibi Hakimeh fields, southwest Iran. In *Carbonate Petroleum Reservoirs* (eds PO Roehl and PW Choquette), pp. 511–23. New York: Springer.

McQuillan H (1991) The role of basement tectonics in the control of sedimentary facies, structural patterns, and salt plug emplacements in the Zagros fold belt of southwest Iran. *Journal of Southeast Asian Earth Sciences* **5**, 453–63.

Misra AA and Mukherjee S (2015) *Tectonic Inheritance in Continental Rifts and Passive Margins*. Berlin: Springer.

Misra AA and Mukherjee S (2018) *Atlas of Structural Geological Interpretation from Seismic Images*. New York: Wiley Blackwell.

Moghadam HS, Stern RJ, Chiaradia M and Rahgoshay M (2013) Geochemistry and tectonic evolution of the Late Cretaceous Gogher–Baft ophiolite, central Iran. *Lithos* **168**, 33–47.

Mohammadrezaei H, Alavi SA, Cardozo N and Ghassemi MR (2020) Deciphering the relationship between basement faulting and two-phase folding in the Hendijan anticline, northwest Persian Gulf, Iran. *Marine and Petroleum Geology* **122**, 104626.

Molinaro M., Guezou JC, Leturmy P, Eshraghi SA and de Lamotte DF (2004) The origin of changes in structural style across the Bandar Abbas syntaxis, SE Zagros (Iran). *Marine and Petroleum Geology* **21**, 735–52.

Motamedi H, Sherkati S and Sepehr M (2012) Structural style variation and its impact on hydrocarbon traps in central Fars, southern Zagros folded belt, Iran. *Journal of Structural Geology* **37**, 124–33.

Motiei H (1994) *Stratigraphy of Zagros*. Tehran: Geological Survey of Iran (in Farsi).

Motiei H (1995) *Petroleum Geology of Zagros*. Tehran: Geological Survey of Iran (in Farsi).

Mouthereau F, Lacombe O and Meyer B (2006) The Zagros folded belt (Fars, Iran): constraints from topography and critical wedge modelling. *Geophysical Journal International* **165**, 336–56.

Mouthereau F, Lacombe O and Vergés J (2012) Building the Zagros collisional orogen: timing, strain distribution and the dynamics of Arabia/Eurasia plate convergence. *Tectonophysics* **532**, 27–60.

Mukherjee S (2011) Estimating the viscosity of rock bodies: a comparison between the Hormuz-and the Namakdan Salt Domes in the Persian Gulf, and the Tso Morari Gneiss Dome in the Himalaya. *Indian Journal Geophysical Union* **15**, 161–70.

Mukherjee S (2014) Review of flanking structures in meso- and micro-scales. *Geological Magazine* **151**, 957–74.

Mukherjee S, Koyi HA and Talbot CJ (2012) Implications of channel flow analogue models in extrusion of the Higher Himalayan Shear Zone with special reference to the out-of-sequence thrusting. *International Journal of Earth Sciences* **101**, 253–72.

Mukherjee S, Talbot CJ and Koyi HA (2010) Viscosity estimates of salt in the Hormuz and Namakdan salt diapirs, Persian Gulf. *Geological Magazine* **147**, 497–507.

Morris P (1977) Basement structure as suggested by aeromagnetic surveys in southwest Iran. *Proceedings of the Second Geological Symposium of Iran*. Tehran: Iranian Geological Institute.

Najafi M, Yassaghi A, Bahroudi A, Vergés J and Sherkati S (2014) Impact of the late Triassic Dashtak intermediate detachment horizon on anticline geometry in the Central Frontal Fars, SE Zagros fold belt, Iran. *Marine and Petroleum Geology* **54**, 23–36.

Najafi M, Vergés J, Etemad-Saeed N and Karimnejad HR (2018) Folding, thrusting and diapirism: competing mechanisms for shaping the structure of the north Dezful Embayment, Zagros, Iran. *Basin Research* **30**, 1200–29.

Noori H, Mehrabi H, Rahimpour-Bonab H and Faghih A (2019) Tectono-sedimentary controls on Lower Cretaceous carbonate platforms of the central Zagros, Iran: an example of rift-basin carbonate systems. *Marine and Petroleum Geology* **110**, 91–111.

O'Brien CAE (1950) Tectonic problems of the oil field belt of southwest Iran. In *Proceedings of the 18th International Geological Congress*, Great Britain, 6, pp. 45–58. Cambridge: Cambridge University Press.

Orang K and Gharabeigli G (2020) Tectonostratigraphic evolution of the Helleh Paleo-high (NW Persian Gulf): insights from 2D and 3D restoration methods. *Marine and Petroleum Geology* **119**, 104443.

Perotti CR, Carruba S, Rinaldi M, Bertozzi G, Feltre L and Rahimi M (2011) The Qatar–South Fars arch development (Arabian Platform, Persian Gulf): insights from seismic interpretation and analogue modelling. In *New Frontiers in Tectonic Research: at the Midst of Plate Convergence* (ed. U Schattner), pp. 325–52. InTechOpen, doi:10.5772/20299.

Pirouz M, Avouac JP, Hassanzadeh J, Kirschvink JL and Bahroudi A (2017) Early Neogene foreland of the Zagros, implications for the initial closure of the Neo-Tethys and kinematics of crustal shortening. *Earth and Planetary Science Letters* **477**, 168–82.

Pla O, Roca E, Xie H, Izquierdo-Llavall E, Muñoz JA, Rowan MG and Huang S (2019) Influence of syntectonic sedimentation and décollement rheology on the geometry and evolution of orogenic wedges: analog modelling of the Kuqa fold-and-Thrust Belt (NW China). *Tectonics* **38**, 2727–55.

Razavi Pash R, Davoodi Z, Mukherjee S, Dehsarvi LH and Ghasemi-Rozveh T (2021a) Interpretation of aeromagnetic data to detect the deep-seated basement faults in fold-thrust belts: NW part of the petroliferous Fars province, Zagros belt, Iran. *Marine and Petroleum Geology* **133**, 105292.

Razavi Pash R, Sarkarinejad K, Sherkati S and Motamedi H (2021b) Analogue model of the Bala Rud Fault, Zagros: an oblique basement ramp in a fold-and-thrust belt. *International Journal of Earth Sciences* **110**(5–6), doi: 10.1007/s00531-021-01987-0.

Reber J, Vidal CS, McLafferty S and Mukherjee S (2021) Relationship between channel flow initiation and crustal viscosity in convergent settings: an analog modelling approach. *International Journal of Earth Sciences* **110**, 2057–64.

Riahi ZT, Sarkarinejad K, Faghih A, Soleimany B and Payrovian GR (2021) Impact of inversion tectonics on the spatial distribution of hydrocarbon traps in the NW Persian Gulf and the southern Dezful Embayment, SW Iran. *Marine and Petroleum Geology* **134**, 105364.

Roma M, Ferrer O, Roca E, Pla O, Escosa FO and Butillé M (2018) Formation and inversion of salt-detached ramp-syncline basins. Results from analog modelling and application to the Columbrets Basin (Western Mediterranean). *Tectonophysics* **745**, 214–28.

Sarkarinejad K and Azizi A (2008) Slip partitioning and inclined dextral transpression along the Zagros Thrust System, Iran. *Journal of Structural Geology* **30**, 116–36.

Sarkarinejad K and Goftari F (2019) Thick-skinned and thin-skinned tectonics of the Zagros orogen, Iran: constraints from structural, microstructural and kinematics analyses. *Journal of Asian Earth Sciences* **170**, 249–73.

Schori M, Zwaan F, Schreurs G and Mosar J (2021) Pre-existing basement faults controlling deformation in the Jura Mountains fold-and-thrust belt: insights from analogue models. *Tectonophysics* **814**, 228980.

Sepehr M and Cosgrove JW (2004) Structural framework of the Zagros fold–thrust belt, Iran. *Marine and Petroleum Geology* **21**, 829–43.

Sepehr M, Cosgrove JW and Moieni M (2006) The impact of cover rock rheology on the style of folding in the Zagros fold-thrust belt. *Tectonophysics* **427**, 265–81.

Setudehnia A (1978) The Mesozoic sequence in south-west Iran and adjacent areas. *Journal of Petroleum Geology* **1**, 3–42.

Sherkati S and Letouzey J (2004) Variation of structural style and basin evolution in the central Zagros (Izeh zone and Dezful Embayment), Iran. *Marine and Petroleum Geology* **21**, 535–54.

Sherkati S, Letouzey J and Frizon de Lamotte D (2006) Central Zagros fold-thrust belt (Iran): new insights from seismic data, field observation, and sandbox modelling. *Tectonics* **25**, TC4007.

Snidero M, Muñoz JA, Carrera N, Butillé M, Mencos J, Motamedi H and Sàbat F (2019) Temporal evolution of the Darmadan salt diapir, eastern Fars region, Iran. *Tectonophysics* **766**, 115–30.

Soleimany B, Poblet J, Bulnes M and Sàbat F (2011) Fold amplification history unraveled from growth strata: the Dorood anticline, NW Persian Gulf. *Journal of the Geological Society* **168**, 219–34.

Stampfli GM and Borel GD (2002) A plate tectonic model for the Paleozoic and Mesozoic constrained by dynamic plate boundaries and restored synthetic oceanic isochrons. *Earth and Planetary Science Letters* **196**, 17–33.

Stewart SA (2018) Hormuz salt distribution and influence on structural style in NE Saudi Arabia. *Petroleum Geoscience* **24**, 143–58.

Stewart SA, Muslem AS and Wibisono G (2018) Triassic fault reactivation in eastern Saudi Arabia: implications for shear and fluid systems on the southern margin of Neotethys. *Journal of the Geological Society* **175**, 619–26.

Stöcklin J (1968) Salt deposits of the Middle East. In *Saline Deposits* (eds RB Mattox and WT Holser), pp. 157–81. Boulder: Geological Society of America, Special Paper no. **88**.

Storti F and McClay K (1995) Influence of syntectonic sedimentation on thrust wedges in analogue models. *Geology* **23**, 999–1002.

Szabo F and Kheradpir A (1978) Permian and Triassic stratigraphy, Zagros basin, south-west Iran. *Journal of Petroleum Geology* **1**, 57–82.

Talbot CJ and Alavi M (1996) The past of a future syntaxis across the Zagros. In *Salt Tectonics*, (eds GL Alsop, DL Blundell and I Davison), pp. 89–109. Geological Society of London, Special Publication no. **100**.

Tavakoli-Shirazi S, Frizon de Lamotte D, Wrobel-Daveau JC and Ringenbach JC (2013) Pre-Permian uplift and diffuse extensional deformation in the High Zagros Belt (Iran): integration in the geodynamic evolution of the Arabian plate. *Arabian Journal of Geosciences* **6**, 2329–42.

Tavani S, Camanni G, Nappo M, Snidero M, Ascione A, Valente E and Mazzoli S (2020) The Mountain Front Flexure in the Lurestan region of the Zagros belt: crustal architecture and role of structural inheritances. *Journal of Structural Geology* **135**, 104022.

Ter Borgh MM, Oldenhuis R, Biermann C, Smit JHW and Sokoutis D (2011) The effects of basement ramps on the deformation of the Prebetics (Spain): a combined field and analogue modelling study. *Tectonophysics* **502**, 62–74.

Tong H, Koyi H, Huang S and Zhao H (2014) The effect of multiple pre-existing weaknesses on the formation and evolution of faults in extended sandbox models. *Tectonophysics* **626**, 197–212.

Vatandoust M, Faghih A, Burberry CM and Shafiei G (2020) Structural style and kinematic analysis of folding in the southern Dezful Embayment oil-fields, SW Iran. *Journal of Structural Geology* **134**, 103989.

Vendeville BC, Ge H and Jackson MPA (1995) Scale models of salt tectonics during basement-involved extension. *Petroleum Geoscience* **1**, 179–83.

Vergés J, Saura E, Casciello E, Fernandez M, Villaseñor A, Jimenez-Munt I and García-Castellanos D (2011) Crustal-scale cross-sections across the NW Zagros belt: implications for the Arabian margin reconstruction. *Geological Magazine* **148**, 739–61.

Warsitzka M, Kley J and Kukowski N (2015) Analogue experiments of salt flow and pillow growth due to basement faulting and differential loading. *Solid Earth* **6**, 9–31.

Weijermars R (1986) Flow behaviour and physical chemistry of bouncing putties and related polymers in view of tectonic laboratory applications. *Tectonophysics* **124**, 325–58.

Withjack MO and Callaway S (2000) Active normal faulting beneath a salt layer: an experimental study of deformation patterns in the cover sequence. *AAPG Bulletin* **84**, 627–51.

Zarifi Z, Nilfouroushan F and Raeesi M (2014) Crustal stress map of Iran: insight from seismic and geodetic computations. *Pure and Applied Geophysics* **171**, 1219–36.

Zebari M, Grützner C, Navabpour P and Ustaszewski K (2019) Relative timing of uplift along the Zagros Mountain Front Flexure (Kurdistan Region of Iraq): Constrained by geomorphic indices and landscape evolution modelling. *Solid Earth* **10**, 663–82.